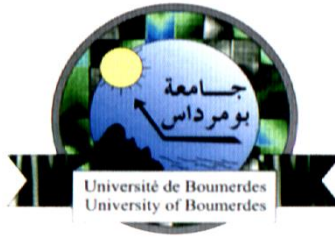**PEOPLE'S DEMOCRATIC REPUBLIC OF ALGERIA**
MINISTRY OF HIGHER EDUCATION AND SCIENTIFIC RESEARCH
UNIVERSITY OF MOHAMED BOUGUERRA BOUMERDES
FACULTY OF SCIENCE AND TECHNOLOGY

Université de Boumerdes
University of Boumerdes

Department of Mechanical Engineering
Energy Installations and Turbomachines

Thesis

Submitted in view of obtaining the Diploma of **Master** Degree**:**

Department of Mechanical Engineering
Energy installation and turbomachine

THEME
Optimizing Thermal Performance of Direct Flow Evacuated Solar Tubes

Presented by: Nesrine BOUBLIA   Mohammed Nabil HAMMADOUCHE
Supervisor: Dr.Samia BOUARABE

University Year: 2023- 2024

Acknowledge:

Abstract:

With the increasing global adoption of renewable energies, including solar energy, direct-flow evacuated solar systems have emerged as highly efficient solutions for thermal energy conversion, maintaining 75% of their efficiency even on overcast days. This thesis aims to enhance the thermal design of these solar collectors and optimize their performance by processing various geometrical, physical, and meteorological data. It examines critical parameters such as solar incident energy ($W \cdot m^{-2}$), absorber length (L in m), mass flow rate ($kg \cdot s^{-1}$), and their impact on the thermal performance of these systems, including efficiency (η), useful heat flux (W), dissipated heat flux (W), and outlet temperature (T_o in K), displaying the results in graphical curves. Utilizing a combination of numerical methods, coding, and simulation, a model of non-linear equations based on heat transfer laws and correlations was developed and solved using the fixed-point method. The results were then compiled and transformed into Fortran code, processed, simulated, and analyzed in Chapter 3. This study provides valuable insights into improving the thermal characteristics and performance of direct-flow evacuated solar collectors, advancing their application in sustainable solar energy systems.

KEYWORDS

ملخص :

مع تزايد الاعتماد العالمي على الطاقات المتجددة، بما في ذلك الطاقة الشمسية، ظهرت أنظمة الطاقة الشمسية المفرغة ذات التدفق المباشر كحل عالي الكفاءة لتحويل الطاقة الحرارية، حيث تحافظ على 75٪ من كفاءتها حتى في الأيام الملبدة بالغيوم. تهدف هذه الأطروحة إلى تعزيز التصميم الحراري لهذا النوع من مجمعات الطاقة الشمسية وتحسين أدائها من خلال معالجة مختلف البيانات الهندسية، الفيزيائية والجوية. تبحث في المعايير الحاسمة مثل الطاقة الشمسية المنبعثة، طول الأنبوب الماص، ومعدل التدفق الكتلي، وتأثيرها على الأداء الحراري لهذه الأنظمة، بما في ذلك الكفاءة، التدفق الحراري المفيد، التدفق الحراري المبدد، ودرجة الحرارة المخرجة، وعرض النتائج في منحنيات رسومية. باستخدام مزيج من الطرق العددية، البرمجة والمحاكاة، تم تطوير نموذج من المعادلات غير الخطية استناداً إلى قوانين وعلاقات انتقال الحرارة، وحُسب باستخدام طريقة النقطة الثابتة. تم جمع النتائج وتحويلها إلى كود فورترون، ومعالجتها، محاكاتها وتحليلها في الفصل الثالث. تقدم هذه الدراسة رؤى قيمة لتحسين الخصائص الحرارية وأداء مجمعات الطاقة الشمسية المفرغة ذات التدفق المباشر، وتعزيز تطبيقها في أنظمة الطاقة الشمسية المستدامة

الكلمات الرئيسية

أنابيب شمسية، تدفق مباشر، سوائل عاملة، الانبوب الماص، نقل حرارة، مفرغة، طريقة النقطة الثابتة، الكفاءة

Résumé :

Avec l'adoption mondiale croissante des énergies renouvelables, y compris l'énergie solaire, les systèmes solaires à évacuation directe sont apparus comme une solution très efficace pour la conversion de l'énergie thermique, maintenant 75% de leur efficacité même par temps couvert. Cette thèse vise à améliorer la conception thermique de ces collecteurs solaires et à optimiser leurs performances en traitant diverses données géométriques, physiques et météorologiques. Elle examine les paramètres critiques tels que l'énergie solaire incidente (W·m⁻²), la longueur de l'absorbeur (L en m), le débit massique (kg·s⁻¹), et leur impact sur la performance thermique de ces systèmes, y compris l'efficacité (η), le flux de chaleur utile (W), le flux de chaleur dissipée (W), et la température de sortie (T_o en K), affichant les résultats dans des courbes graphiques. En utilisant une combinaison de méthodes numériques, de codage et de simulation, un modèle d'équations non linéaires basé sur les lois et les corrélations de transfert de chaleur a été développé et résolu en utilisant la méthode du point fixe. Les résultats ont ensuite été compilés et transformés en code Fortran, traités, simulés et analysés dans le chapitre 3. Cette étude fournit des informations précieuses pour améliorer les caractéristiques thermiques et les performances des collecteurs solaires à évacuation directe, faisant progresser leur application dans les systèmes d'énergie solaire durable.

MOTS-CLÉS

Tubes solaires, flux direct , fluides de travail , absorbeur , transfert de chaleur , évacué , méthode à point fixe , efficacité.

Content

List of figures

Figure 18: The outlet temperature versus the absorber length for different values of the incident radiation flux density.

Figure 19: The useful heat flux versus the absorber length for different values of the incident radiation flux density.

Figure 20: The dissipated heat flux versus the absorber length for different values of the incident radiation flux density.

Figure 21: The efficiency versus the absorber length for different values of the incident radiation flux density.

Figure 22: The outlet temperature versus the incident radiation flux density for different values of the mass flow.

Figure 23: The useful heat flux versus the incident radiation flux density for different values of the mass flow.

Figure 24: The dissipated heat flux versus the incident radiation flux density for different values of the mass flow.

Figure 25: The efficiency versus the incident radiation flux density for different values of the mass flow.

List of tables

Nomenclature

Nomenclature

Latin Lettres

Symbole	Designation	Unity
C	the heat capacity	$J.K^{-1}$
F	view factor, also called the shape factor	
G	the gravitational acceleration due to earth	$m.S^{-1}$
G	the solar incident flux	$W. m^{-2}$
L	a representative dimension of the physical domain	m
m	mass flow	$KG^{-1}.S^{-1}$
r	the radius of geometry	m
S	the cross-sectional area	m^2
S	the area of the emitting surface	m^2
S	the surface area of the object	m^2
T	the temperature	K
T	temperature of the emitting surface	K
t	The time	S
Ts	the temperature of the object	K
T_∞	the temperature of the surroundings	K
V	the average velocity of the fluid	$m.S^{-1}$

Greek Lettres

Symbol	Designation	Unite
$\overline{grade}$	Gradient	
α	the diffusivity	$m^{-2}.S^{-1}$
$\tau\alpha$	the transmissivity	
β	the thermal expansion coefficient	K^{-1}
φ	Angle	Rad
φ	the rate of heat transfer per unit	W
Ө	angle	Rad
P	the density of material	Kg/m^3
λ	the thermal conductivity	$W.m^{-1}.K^{-1}$
δ	declination	degree
Φ	the heat flux	W
Φ	the heat transfer coefficient	$W.m^{-2}.K^{-1}$
ν	the cinematic viscosity	$m^2.S^{-1}$
ε	the emissivity of the material	
σ	the constant of Stefan-Boltzmann	$W.m^{-2}.K^{-4}$

Adimensionnel   Numbers

Symbol   Désignation

Re   Reynolds Numbre
N$_u$ Nusselt Numbre
Gr   Grachouff Numbre
Pr   Prandtl number

Indices

Symbol   Designation   Unity

A   absorbeur
Ao   outer absorbeur
Ai   inner absorbeur
Hrd   the radiative heat coefficient $W.K^{-1}$
Hcd   the conductive heat coefficient $W.K^{-1}$
Hcv   the convective heat coefficient $W.K^{-1}$
Hgh   the global heat coefficient $W.K^{-1}$
Tev   temperature of the environment   K
Tai   the inner temperature of the absorbeur   K
Tao   the uter temperature of the absorbeur   K
Tci   the inner temperature of the cover   K
Tco   the outer temperature of the cover   K
Tft   the inlet temperature of the working   K
Tfo   the outlet temperature of the working   K
Sao   outer absorbeur surface   m^2
Sai   inner absorbeur surface   m^2

General Introduction

Introduction

Substantial energies come from natural resources that are replenished over time, such as sunlight, wind, rain, tides, and geothermal heat. These sources of energy are considered renewable because they are continually replenished and will not run out like finite resources such as fossil fuels. Renewable energy is becoming increasingly important as the world seeks to reduce greenhouse gas emissions and mitigate the impacts of climate change. Substantial energies are becoming more affordable and widespread, and they have the potential to provide a significant portion of the world's power needs.

There are several types of renewable energy such as solar energy which is collected from the sun using technologies like solar panels or concentrating solar power systems. The wind energy which is provided from the wind motion using wind turbines. Wind energy is one of the fastest growing sources of renewable energy. The geothermal energy which is an energy that is harnessed from the earth's heat. The biomass energy which is generated from organic matter such as wood, crops, and wastes.

However, there are still challenges to overcome, such as intermittency and the need for energy storage, to fully realize the potential of renewable energy.

Solar collectors are devices that capture and convert sunlight into usable energy, typically in the form of heat or electricity. There are several types of solar collectors, including flat-plate collectors which are the most common type of solar collectors and are typically used for heating water and Concentrated solar power (CSP) systems which are large-scale solar power plants that use mirrors or lenses to concentrate sunlight onto a small area, generating high temperatures that can be used to produce steam and generate electricity. There are also Photovoltaic (PV) collectors which are devices that convert sunlight directly into electricity through the use of semiconducting materials such as silicon. They are commonly used in residential and commercial solar panel installations.

Solar collectors have several advantages, including their low operating costs and their environmental friendliness, as they generate electricity without producing harmful greenhouse gases. However, their efficiency depends on various factors, such as weather conditions and the angle and orientation of the collector, and they may not always be suitable for all applications or locations.

In the present work, we will initially in the first chapter discuss in detail the three mechanisms of the heat transfer which are the conduction, the convection and radiation where we provide their underlying physics as well as their algebraic formalisms required for the modeling of the direct flow evacuated solar collector.

The second chapter will be focused the construction of a reliable mathematical model able to furnish accurate outcomes as the thermal efficiency, the outlet temperature of the working fluid, the useful flux and the dissipated flux. The mathematical model has been built basing on different realistic assumptions that led a system of highly and coupled nonlinear algebraic equations where the fixed-point method had been applied to flexibly solve the problem.

The last chapter will be totally centered on the results and their interpretations where we commence by discussing the fixed-point method and its convergence criteria then we deliver indispensable graphs that allow us a better understanding and consequently a high monitoring and optimization of this specific kind of solar device.

Chapter I
Heat transfer,
An overview

Chapter I Heat transfer: An overview

Introduction:

Heat transfer refers to the movement of thermal energy from one body or system to another. This energy can be transferred by conduction, convection, or radiation. We introduce in the present chapter a variety of physical concepts and mathematical formalisms that deal with the three heat transfer processes, including the conduction, convection and radiation, which are a key element in the calculation and thermal design in the field of solar thermal conversion technology, usually performing by flat plate collectors, solar concentrators and evacuated solar tubes. We initially start by providing general definitions about the conduction heat transfer while we give the important physical notions as well as the governing equations needed for the calculations. We then discuss the heat transfer by both natural and forced convection as well as the techniques employed in the determination of the heat transfer coefficient. We finally undertake the radiation heat mechanism by providing the necessary theoretical concepts requiring for the modeling of the evacuated solar tube such as Stefan-Boltzmann laws well as essential formulae for evaluating of net radiative heat exchange between surfaces.

I.1 Conduction

Conduction is one of the three modes of heat transfer, and it refers to the transfer of heat energy between objects in direct contact with each other or through the object itself by phonons (vibrations of the inside the object crystal lattice). In conduction, thermal energy is transferred from the hotter object to the cooler object, causing a decrease in temperature of the hotter object and an increase in temperature of the cooler object to increase until a thermal balance will take place leading to equalization to both temperatures [1].
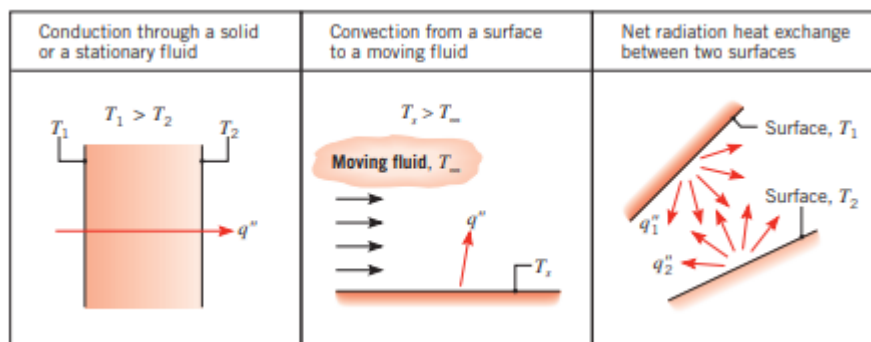
Figure 1. Conduction, convection, and radiation heat transfer modes [2].

I.1.1 Fourier law

Fourier's Law is a fundamental principle in physics that describes the flow of heat between two objects or regions with different temperatures. It states that the rate of heat transfer through a material is proportional to the temperature gradient (the rate of change of temperature with coordinates) and a constant of proportionality known as the thermal conductivity. The law can be expressed mathematically as [3]

$$\phi = -\lambda S \vec{n}\, \overrightarrow{grad}T \qquad (1)$$

While

$\overrightarrow{grad}T$: is the gradient of the temperature, defined by

$$\overrightarrow{grad}T = \frac{\partial T}{\partial x}\vec{i} + \frac{\partial T}{\partial y}\vec{j} + \frac{\partial T}{\partial z}\vec{k} \qquad (2)$$

Where

(i, j, k): are unit vectors.

$\vec{n}$: is a normal vector.

(x, y, z): are the coordinates in m.

T: is the temperature in K.

S: is the cross-sectional area in m^2.

λ: is the thermal conductivity in $W. m^{-1}. K^{-1}$.

ϕ: is the heat flux in W.

The above equation can be used to calculate the rate of heat transfer in a variety of situations, such as in the design of building insulation, the cooling of electronic devices, or the heating and cooling of industrial processes [3].

I.1.2 Thermal conductivity

Thermal conductivity is a material property that describes how well a material conducts heat. It is defined as the amount of heat energy that can be transferred through a unit area of a material in a unit of time, per unit temperature gradient. In other words, thermal conductivity is a measure of the rate at which heat flows through a material [3].

Materials with high thermal conductivity allow heat to flow easily and speedily through them, while materials with low thermal conductivity are poor conductors of heat. Metals, such as copper and aluminum, have high thermal conductivity, while materials like wood and plastics have lower thermal conductivity [3] [4].

In some cases, the thermal conductivity is assumed to be function of temperature. However, for the sake of simplicity during numerical calculation, we consider that the thermal conductivity is independent of temperature. Table **1**, provides data for the thermal conductivity for different materials [4].

Table 1: Thermal conductivity for different materials [4]

Materials	$\lambda\ in\ W.m^{-1}.K^{-1}$	**Materials**	$\lambda\ in\ W.m^{-1}.K^{-1}$
Water	0.6	Engin oïl	0.15
Glass	0.81	Fréon	0.04
Copper	399	Hydrogen	0.18
Aluminium	237	Air	0.026
Carbon Steel	43	Ice	1.6
Plastics	0.2-0.3	Wood	0.04-0.12
Ethylene glycol	0.26	Gold	310

I.1.3 Conduction equation

The conduction equation is a fundamental tool in the study of heat transfer which is used in a variety of applications, such as the analysis of heat transfer in materials, the design of heat exchangers, and the simulation of thermal processes in engineering and physics. The conduction equation is a partial differential equation that describes the transfer of heat through a material

by conduction. It is also known as the heat diffusion equation and can be written in various coordinates system as [5]

I.1.3.1 Conduction equation in Cartesian coordinates

The heat equation is expressed in Cartesian coordinates as

$$\frac{\partial T}{\partial t}\frac{1}{a} = \frac{\partial^2 T}{\partial x^2} + \frac{\partial^2 T}{\partial y^2} + \frac{\partial^2 T}{\partial z^2} \qquad (3)$$

I.1.3.2 Conduction equation in cylindrical coordinates

The heat equation is expressed in cylindrical coordinates as

$$\frac{1}{r}\frac{\partial}{\partial r}\left(r\frac{\partial T}{\partial r} \right) + \frac{1}{r^2}\frac{\partial^2 T}{\partial \phi^2} + \frac{\partial^2 T}{\partial z^2} = \frac{1}{a}\frac{\partial T}{\partial t} \qquad (4)$$

I.1.3.3 Conduction equation in spherical coordinates

The heat equation is expressed in spherical coordinates as

$$\frac{1}{r}\frac{\partial}{\partial r}\left(r\frac{\partial T}{\partial r} \right) + \frac{1}{r^2 \sin^2 \theta}\frac{\partial^2 T}{\partial \varphi^2} + \frac{1}{r^2 \sin^2 \theta}\frac{\partial}{\partial \theta}\left(\sin \theta \frac{\partial^2 T}{\partial \theta} \right) = \frac{1}{a}\frac{\partial T}{\partial t} \qquad (5)$$

Where

t : is the time in s.

r : is the radius of geometry in m.

φ, θ : are the angles in rad.

a : is the diffusivity in $m^{-2}.s^{-1}$.

It should be noted that the thermal diffusivity is a material property that measures how quickly a material can transfer heat through it. It is given by the following formula [2]

$$a = \frac{\lambda}{\rho c} \qquad (6)$$

Where

ρ : is the density of material in $Kg.m^{-3}$.

c : is the heat capacity of material in $J.Kg^{-1}.K^{-1}$.

I.2 Convection

Convection is a process of heat transfer that occurs in fluids (liquids and gases) when there is a temperature difference within the fluid. It is the transfer of heat by the movement of mass or energy from one place to another, depending also on the physical geometry.

In natural convection, the fluid motion is caused by buoyancy forces that result from the difference in density of the fluid due to the temperature gradient. Hot fluids become less dense and rise, while cooler fluids become denser and sink. This creates a circulation that carries energy from hotter regions to cooler regions. Whereas forced convection, the fluid motion is created by an external force, such as a pump or a fan. The external force causes the fluid to move, which can enhance the heat transfer process.

Convection is a very important process in many natural and industrial systems. For example, it plays a critical role in atmospheric circulation, ocean currents, and the cooling of electronic devices. Convection is also used in various industrial processes, such as in cooling towers, heat exchangers, and in the heating and ventilation of buildings [5].

I.2.1 Newton law

The convection Newton Law, also known as Newton's law, describes the rate of heat transfer between an object and its surroundings through convection. It states that the rate of heat transfer is proportional to the temperature difference between the object and its surroundings and a constant of proportionality called the convection heat coefficient [3].

The mathematical expression of the Convection Newton Law is:

$$\varphi = hS(T_\infty - T_S) \tag{7}$$

Where

φ : Is the rate of heat transfer per unit time

h : is the heat transfer coefficient in $W.m^{-2}.K^{-1}$.

S : Is the surface area of the object in m^2.

T_s : Is the temperature of the object in K.

T_∞ : Is the temperature of the surroundings in K.

This law is commonly used in many applications, including heating and cooling systems, cooking, and many other areas where heat transfer is important.

I.2.1.1 Convection heat transfer coefficient

The convection heat transfer coefficient h is a measure of how effectively a fluid, such as air or water, transfers heat by convection from a solid surface to the fluid. It represents the rate of heat transfer per unit area of the solid surface per unit temperature difference between the solid surface and the fluid. The convection heat transfer coefficient depends on various factors such as the fluid properties (density, viscosity, and thermal conductivity), the flow velocity of the fluid, the geometry and surface roughness of the solid surface, and the temperature difference between the solid surface and the fluid. The value of the convection heat transfer coefficient h can be determined experimentally combining with theoretical analysis to formulate different useful correlations in terms of Nusselt number for natural and forced convections as [6]

$$Nu = h\frac{L}{\lambda} \qquad (8)$$

Where

L : Is a representative dimension of the physical domain in m.

I.2.2 Natural convection

Natural convection is a type of heat transfer in which fluid motion is driven solely by buoyancy forces that arise from temperature differences within the fluid. It occurs when a fluid, such as a gas or a liquid, is heated, causing its density to decrease and it to rise, while cooler fluid sinks to take its place. The rate of natural convection is influenced by many factors, such as the geometry of the system, the temperature difference between the hot and cold regions, and the properties of the fluid, such as its viscosity and thermal conductivity. These factors can be modeled mathematically using fluid mechanics and thermodynamics to predict the heat transfer rate and optimize the design of natural convection systems [6].

In the natural convection the Nusselt number Nu itself is experimentally determined as a function of the Grashof number Gr and the Prandtl number Pr according to the geometry as [2]

$$Nu = f(Gr; Pr) \qquad (9)$$

Where Grashof number and Prandtl number are defined respectively as

$$Gr = \frac{g\beta(T_\infty - T_S)L^3}{v^2} \qquad (10)$$

And

$$Pr = \frac{v}{a} \qquad (11)$$

Where

g : is the gravitational acceleration due to earth in $m.s^{-2}$.

β : is the thermal expansion coefficient in K^{-1}.

v : is the cinematic viscosity in $m^2.s^{-1}$.

a : is the diffusivity of the fluid viscosity in $m^2.s^{-1}$.

For natural convection, Table **2** provides useful correlations of the Nusselt number Nu for an outer surface of an inclined cylinder.

Table 2: Correlation for Nusselt number for natural convection [7] [8].

Author	Correlation	L/D	Pr
Sed Ahmed and Shemilt	$Nu_L = 0.498(Ra_L \cos\phi)0.28$ $1.9 \times 10^{10} < Ra_L \cos\phi < 3.8 \times 10^{11}$	4.65−14	2300
Al-Arabi and Salman	$Nu_L = \left[0.6 - 0.488(\sin(90 - \varphi))^{1.73}\right] Ra_L^{\frac{1}{4} + \frac{1}{22}(\sin-(90-\varphi))1.73}$ $10^{55} < Ra_L < 10^7$	25	0.7
Oosthuizen	$\dfrac{Nu}{(Gr \times \cos\phi)^{\frac{1}{4}}} = 0.42\left[1 + \left(\dfrac{1.31}{L^{\frac{-1}{4}}}\right)^3\right]^{\frac{1}{2}}$ $\bar{L} = \dfrac{L}{D \tan\phi}, \quad 10^4 < Ra_d < 10^9$	8,10, 16	0.7
Stewart and Buck	$\dfrac{Nu}{(Ra \times \cos\phi)^{\frac{1}{4}}} = 0.48 + 0.555\left(\left(\dfrac{D}{L \times \cos\phi}\right)^{\frac{1}{4}} + \left(\dfrac{D}{L}\right)^{\frac{1}{4}}\right)$	6, 9, 12	0.7

I.2.2 Forced convection

During forced convection, the heat transfer is directly proportional to the velocity of the fluid, the surface area of the object, and the temperature difference between the fluid and the object. The heat transfer is also influenced by the properties of the fluid, such as its density, viscosity, and thermal conductivity. The Nusselt number in this situation is expressed in terms of the Reynolds number Re and the Prandtl number Pr as [4]

$$Nu = f(\text{Re}; \text{Pr}) \qquad (12)$$

The Reynolds number is given by

$$Re = \frac{Vl}{\nu} \qquad (13)$$

Where

V : is the average velocity of the fluid in $m.s^{-1}$.

Table 3: Correlation of the Nusselt number Nu for an inner surface of an inclined cylinder experimental results [9].

$$Nu = c\,Re^n \qquad (13)$$

Cylinder position	C	n	Reynolds number
incline	0.1686	0.6971	$8900 < Re < 48000$

Table 4: Correlation for Nusselt number for forced convection [10]

Authors	Correlations
Dittus-Boelter	$Nu = 0.023\,Re^{0.8}\,Pr^{0.4}$
Churchill-Chu	$Nu = \dfrac{\left(0.60 + 0.387\,Re^{0.5}\right)}{\left(1 + \left(\left(\dfrac{0.559}{Pr}\right)^{0.9}\right)^{0.5}\right)^2}$
Gnielinski	$Nu = \left(\dfrac{f}{8}\right)\left(\dfrac{(Re - 1000)Pr}{\left(1 + 12.7\left(\dfrac{f}{8}\right)^{0.5}\left(Pr^{\frac{2}{3}} - 1\right)\right)}\right)$
Gnielinski	$Nu = \left(\dfrac{f}{2}\right)\left(\dfrac{Re\,Pr}{\left(1 + 1.12\left(\dfrac{f}{2}\right)^{0.5}\left(Pr^{\frac{2}{3}} - 1\right)\right)}\right)$
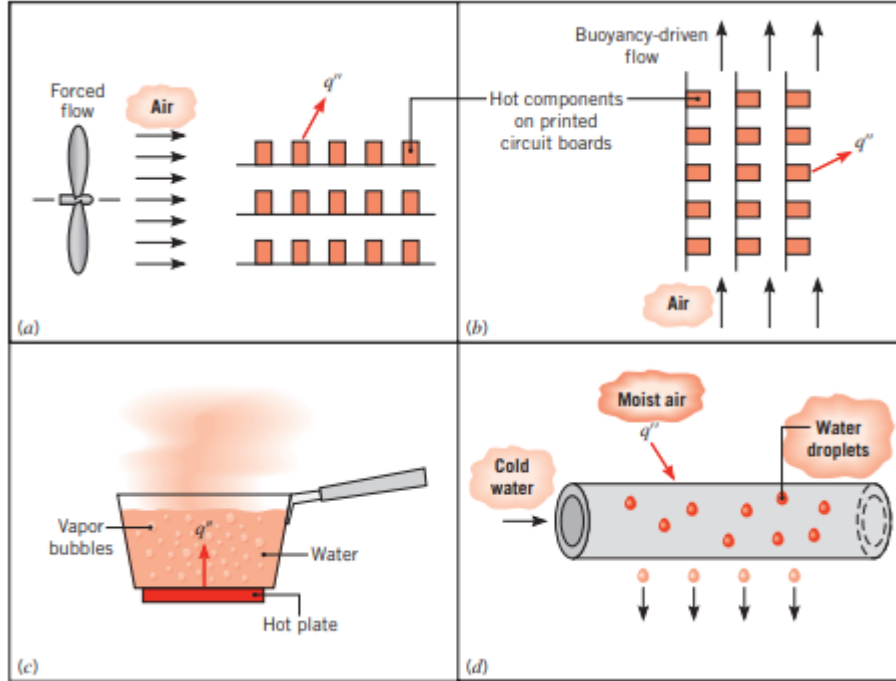
Figure 2. Convection heat transfer processes. (a) Forced convection. (b) Natural

convection. (c) Boiling. (d) Condensation [1].

I.3 Radiation

Radiation heat transfer is the transfer of thermal energy in the form of electromagnetic waves, without the need for a physical medium to transfer the energy. This type of heat transfer occurs between any two surfaces that are at different temperatures and is independent of any intervening material. Radiation heat transfer occurs in all directions and can travel through a vacuum. Radiation heat transfer is governed by the Stefan-Boltzmann law, which states that the rate of heat transfer by radiation is proportional to the fourth power of the absolute temperature difference between two surfaces [2] [11].

I.3.1 Stefan-Boltzmann law

The Stefan-Boltzmann is given by the following equation as [4]

$$\varphi = S\varepsilon\sigma T^4 \qquad (14)$$

Where

φ : Is the rate of heat transfer in W.

ε : Is the emissivity of the material which is dimensionless,

S : is the area of the emitting surface in m^2.

T : Is temperature of the emitting surface in K.

$\sigma = 5.67 \times 10^{-8}$: Is the constant of Stefan-Boltzmann in $W.m^{-2}.K^{-4}$.

It should be pointed out that the emissivity of a material ε is a measure of its ability to emit radiation and is given a value between 0 and 1. A material with an emissivity of 1 is a perfect emitter of radiation, while a material with an emissivity of 0 does not emit any radiation [4].

Table 5: Emissivity for different materials [12].

Surface Materials	Emissivity Coefficient	Surface Materials	Emissivity Coefficient	Surface Materials	Emissivity Coefficient
Water 0-100∘c	0.95– 0.963	Black paint on metallic substrate	0.97	Cement	0.57
evaporated aluminum film	0.03	Red brick	0.93	Cotton cloth	0.77
Fused quartz on aluminum film	0.81	Human skin	0.97	Glass	0.92-0.97
White paint on metallic substrate	0.96	Snow	0.97	Plastics	0.90-0.97
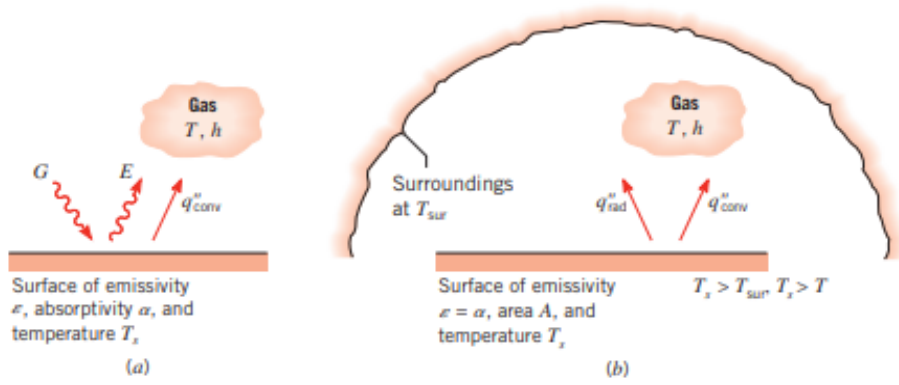
Figure 3. Radiation exchange: (a) at a surface and (b) between a surface and large surrounding [1].

I.3.2 Radiative heat exchange between two surfaces

Radiative heat exchange is the transfer of thermal energy between two surfaces that are at different temperatures through electromagnetic radiation. This type of heat transfer does not require a medium or a physical contact between the surfaces. Instead, the surfaces exchange energy by emitting and absorbing thermal radiation [2] [20], see figure **4**.
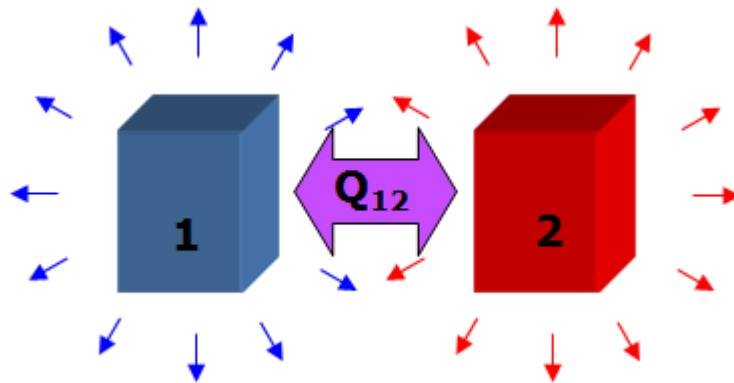
Figure 4. Radiative heat exchange between two surfaces.

The next radiative heat exchange is given by the following formula [6] as

$$\varphi_{1-2} = \frac{\sigma(T_1 - T_2)^4}{\dfrac{1-\varepsilon_1}{S_1\varepsilon_1} + \dfrac{1}{S_1 F_{1-2}} + \dfrac{1-\varepsilon_2}{S_2\varepsilon_2}} \qquad (15)$$

Where

φ_{1-2} : is the amount of radiative heat emitted by the surface 1 and absorbed by the surface 2 in W.

F_{1-2} : is view factor, also called the shape factor.

The View Factor is the portion of the radiative heat flux which leaves surface A that strikes surface B. In simpler terms, the view factor measures how well one surface can see another surface [1] [6]. View factors are purely geometrical parameters and are independent of the physical surface properties and temperature, see figure **5**.
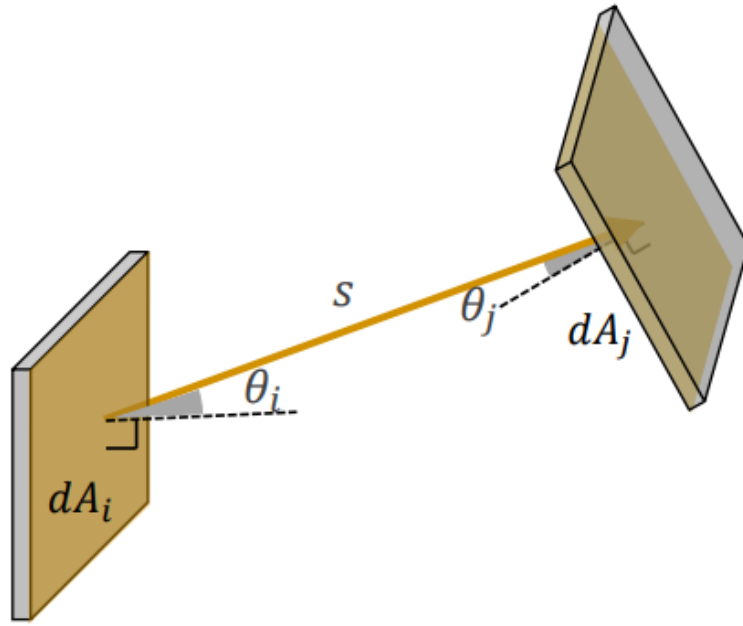
Figure 5 : View factor

It is defined in the integral form as

$$dF_{i-j} = \frac{1}{S_i} \int_{S_I} \int_{S_J} \frac{(\cos\theta_i \ \cos\theta_j)}{\pi L} dS_i dS_j \qquad (16)$$

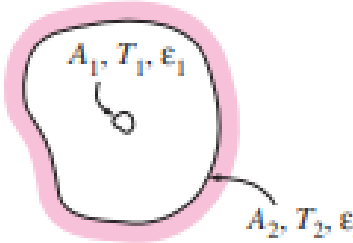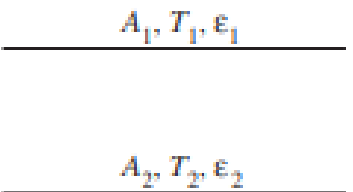In most case, equation (15) is evaluated numerically [2] [6].
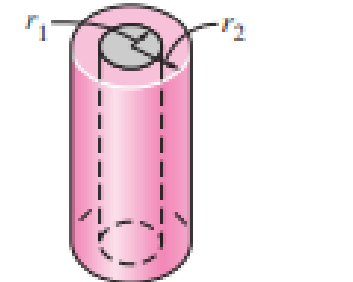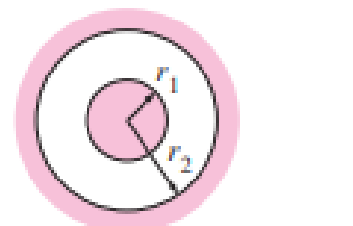
While both quantities are also defined as

$$\varphi_{1-2} = -\varphi_{2-1} \qquad (17)$$

And

$$S_1 F_{1-2} = S_2 F_{2-1} \qquad (18)$$

Table 6: View factor for different radiative surface configurations [13]

Small object in a large cavity		
A_1, T_1, ε_1 A_2, T_2, ε_2	$\dfrac{A_1}{A_2} \approx 0$ $F_{12} = 1$	$\dot{Q}_{12} = A_1 \sigma \varepsilon_1 (T_1^4 - T_2^4)$
Infinitely large parallel plates		
A_1, T_1, ε_1 A_2, T_2, ε_2	$A_1 = A_2 = A$ $F_{12} = 1$	$\dot{Q}_{12} = \dfrac{A\sigma(T_1^4 - T_2^4)}{\dfrac{1}{\varepsilon_1} + \dfrac{1}{\varepsilon_2} - 1}$
Infinitely long concentric cylinders		
r_1 r_2	$\dfrac{A_1}{A_2} = \dfrac{r_1}{r_2}$ $F_{12} = 1$	$\dot{Q}_{12} = \dfrac{A_1 \sigma(T_1^4 - T_2^4)}{\dfrac{1}{\varepsilon_1} + \dfrac{1-\varepsilon_2}{\varepsilon_2}\left(\dfrac{r_1}{r_2}\right)}$
Concentric spheres		
r_1 r_2	$\dfrac{A_1}{A_2} = \left(\dfrac{r_1}{r_2}\right)^2$ $F_{12} = 1$	$\dot{Q}_{12} = \dfrac{A_1 \sigma(T_1^4 - T_2^4)}{\dfrac{1}{\varepsilon_1} + \dfrac{1-\varepsilon_2}{\varepsilon_2}\left(\dfrac{r_1}{r_2}\right)^2}$

Consclusion:

The present chapter has been dealing with the three heat transfer processes occurring during the energy conversion inside the different thermal collectors. We have provided the most elementary theoretical basis that leads the construction of a reliable mathematical model for the numerical calculation of different thermal performance of an evacuated solar tube including the outlet temperature and the efficiency.

Chapter II
Evacuated solar tube: Thermal design

Chapter II Evacuated solar tube: Thermal design

The present chapter is devoted to the construction of a consistent mathematical model for an evacuated solar tube that aims to the calculation and prediction of the thermal performance by including different geometrical, physical and meteorological data that may influence the overall needed outcomes of thermal collector in question. We first begin by a detailed description of the evacuated solar tube as an efficient thermal converter of the incident solar irradiation into useful heated water by invoking its working principle and the materials used in each one of its components. We then build the set of the algebraic equations under on certain physical assumptions and basing on thermal balances of the different heat exchanges inside and outside the evacuated tube, a feature that allows the determination of thermal performance. Finally, we provide a flowchart allowing the numerical assessment of the of efficiency and of the outlet temperature as a function of different physical input.

II.1 Evacuated solar tubes: working principle, components and materials

An evacuated solar tube is a type of solar thermal collector used to capture and convert solar energy into heat. It is commonly used for domestic hot water systems, space heating, and industrial processes. The collector consists of a series of parallel, transparent glass tubes that are evacuated of air, leaving a vacuum between the inner and outer tubes. The inner tube is coated with a selective absorber material that absorbs solar radiation and converts it into heat. The vacuum between the tubes acts as an insulator, minimizing heat loss and maximizing the efficiency of the collector, table **7** cites different kind of vacuum in terms of pressure. When solar radiations enter the evacuated tube, it is absorbed by the selective coating on the inner tube, which heats up and transfers the heat to a fluid flowing through the tube. The fluid can be either water or a heat transfer fluid such as antifreeze [14]. The heated fluid is then circulated through a heat exchanger, transferring its heat to a storage tank or the building's heating system, see figure **6**.
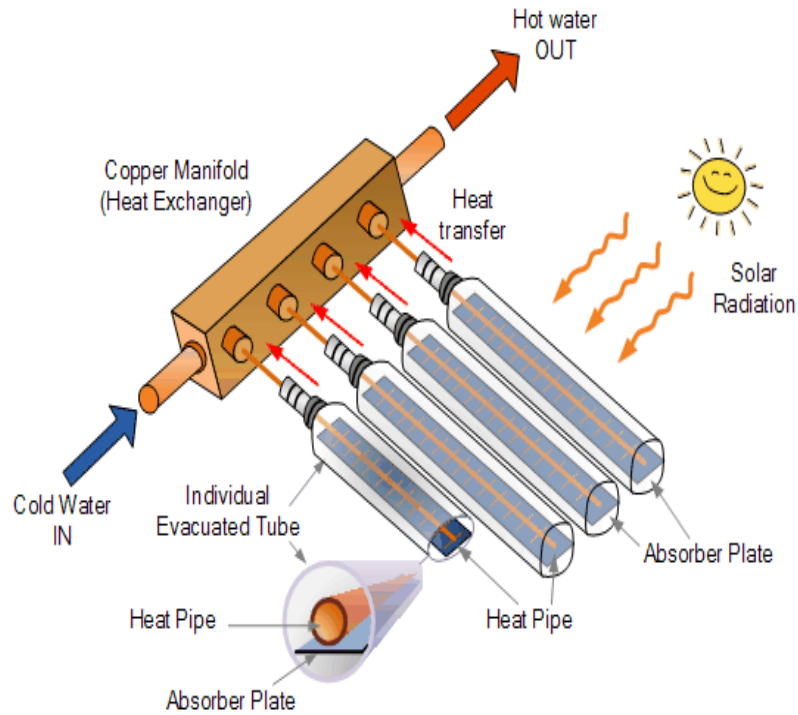
Figure 6: Schematic representation of an evacuated solar tube

When solar radiations enter the evacuated tube, it is absorbed by the selective coating on the inner tube, which heats up and transfers the heat to a fluid flowing through the tube. The fluid can be either water or a heat transfer fluid such as antifreeze. The heated fluid is then circulated through a heat exchanger, transferring its heat to a storage tank or the building's heating system.

Table 7 Degrees of vacuum and vacuum levels for industrial and laboratory applications [16].

Types of vacuum	Degree in Torr
Perfect vacuum	0
Outer space	10^{-9}– 10^{-17} Torr
Extreme high vacuum	Around 10^{-13} Torr
Ultra high vacuum	10^{-10}– 10^{-11} Torr
High vacuum	10^{-5}– 10^{-8} Torr
Medium vacuum	10^{-3}– 10^{-5} Torr
Low vacuum	Around 10^{-3} Torr
Atmospheric vacuum	Around 760 Torr

II1.1 Heat pipe evacuted solar tube

A heat pipe evacuated solar tube is a type of solar collector used to harness solar energy for heating purposes. It consists of a glass tube that is evacuated (meaning that the air is removed from the tube to create a vacuum) and contains a heat pipe. The heat pipe is a sealed copper tube that contains a small amount of liquid, such as water or alcohol, that has a low boiling point. When the solar radiations enter the evacuated tube, they are absorbed by an inner layer of metal or ceramic coating on the tube, which heats up and transfers the heat to the heat pipe. The heat causes the liquid inside the heat pipe to boil, and the resulting vapor rises to the top of the heat pipe, where it condenses back into liquid and releases its heat. This heat is then transferred to a heat transfer fluid (such as water or glycol) that circulates through a heat exchanger in the solar collector, which can then be used for heating water or space [14]. The use of an evacuated tube with a heat pipe allows for efficient transfer of solar energy into heat, even in cold or cloudy conditions, as the vacuum inside the tube minimizes heat loss to the surrounding environment. This technology is commonly used in solar water heating systems for residential and commercial buildings, see figure **7**.
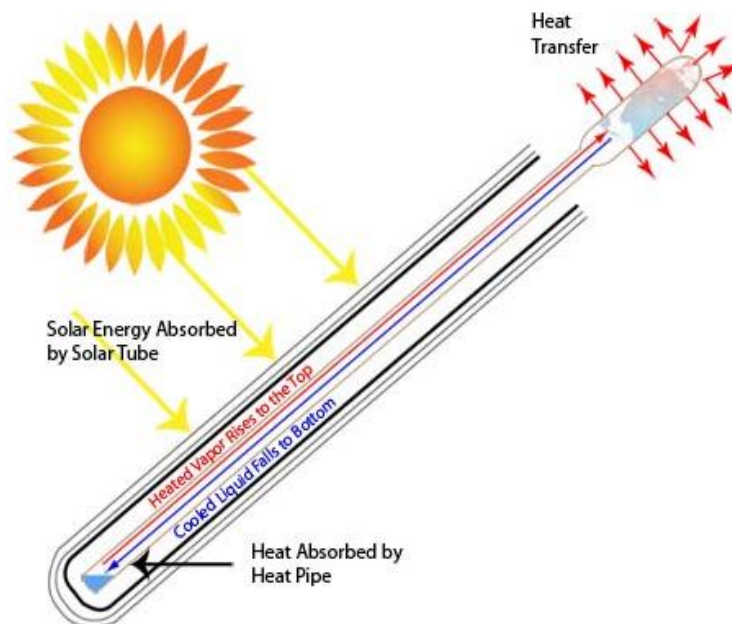
Figure 7: Schematic representation of heat pipe evacutaed solar tube

II1.2 Direct flow evacutaed solar tube

Direct flow evacuated tube collectors are a type of solar thermal technology used for capturing and converting solar energy into heat for various applications such as hot water heating, space heating, and industrial processes. In a direct flow system, the heat transfer fluid (usually water or a mixture of water and antifreeze) is circulated directly through the tubes to absorb the heat energy and carry it away to a storage tank or other heat exchanger. The fluid is pumped through the tubes continuously while the sun is shining, and when the fluid reaches the desired temperature, it is then used for its intended purpose. Direct flow evacuated tube collectors are highly efficient and can achieve high temperatures even in colder climates, making them suitable for a wide range of applications. They are also lightweight, durable, and easy to install, making them a popular choice for residential and commercial buildings, as well as industrial facilities, see figure **8**.
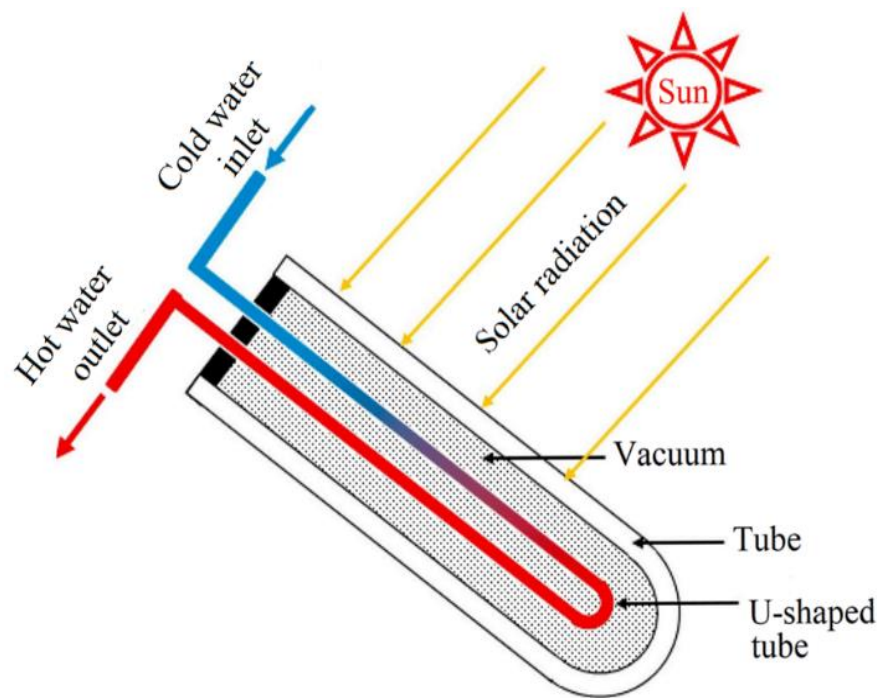
Figure 8: Schematic representation of direct flow evacutaed solar tube

Remark

One advantage of both evacuated tube collectors is their high efficiency, as the vacuum insulation reduces heat loss and the selective absorber coating maximizes solar absorption. They also perform well in cold and cloudy conditions, as the vacuum insulation prevents heat loss due to convection and radiation. However, evacuated tube collectors are typically more expensive than other types of solar thermal collectors, and their vacuum tubes are fragile and can break easily if mishandled [11] [14]. They also require regular maintenance to ensure proper functioning and longevity.

II.2 Thermal design

We will describe and evaluate in what follows the absorbed, useful, dissipated heat fluxes as well as the efficiency of the evacuated solar collector that represent key parameters in solar thermal design.
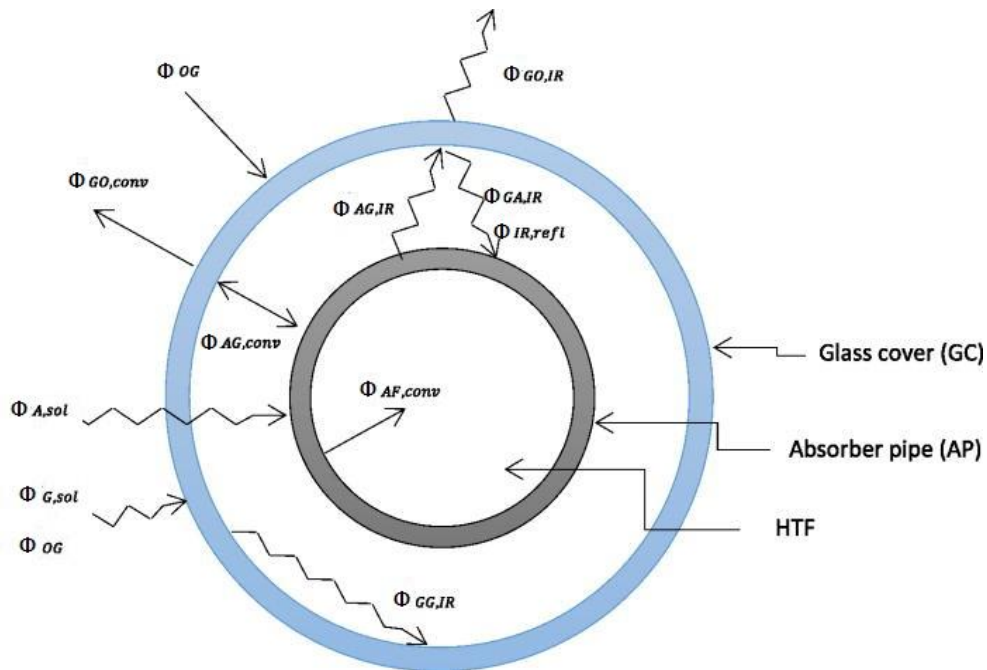
Figure 9: Schematic representation of heat exchanges between the receiver surfaces and the outside environment [15].

II.2.1 Determination of the efficiency of evacuated solar collector

The detailed analysis of a solar collector is a complicated problem. Fortunately, a relatively simple analysis will yield very useful results. These results show the important variables, how they are related, and how they affect the performance of a solar evacuated collector.

To illustrate these basic principles, we absolutely need adopt the following simplifying assumptions:

1. The heat flow through the inclined cylindrical cover (envelope) is one dimensional. Assuming constant temperatures simplifies the analysis by eliminating the need to account for temperature variations over time. While in reality, temperatures may fluctuate, this assumption allows us to focus on the steady-state behavior of the system, which is often sufficient for practical purposes.

2. The Outer and inner temperature of both cover and absorber are maintained constant. Assuming constant temperatures simplifies the analysis by eliminating the need to account for temperature variations over time. While in reality, temperatures may fluctuate, this assumption allows us to focus on the steady-state behavior of the system, which is often sufficient for practical purposes.

3. The thermal properties of the cover and absorber are independent of temperature. This assumption simplifies the calculations by treating the thermal properties of the cover and absorber materials as constant values. While thermal properties can vary with temperature, especially for certain materials, assuming constant properties allows us to use simplified equations and avoid complex temperature-dependent calculations.

4. The environment temperatures radiation and convection are not equal. Distinguishing between radiation and convection simplifies the analysis by recognizing the different mechanisms through which heat transfer occurs between the collector and its surroundings. Radiation involves energy transfer through electromagnetic waves, while convection involves the transfer of heat through fluid motion. Treating them separately helps in accurately modeling the heat exchange processes.

5. The effect of dust and dirt on the evacuator collector is negligible. This assumption simplifies the analysis by ignoring the impact of dust and dirt accumulation on the performance of the collector. While in real-world scenarios, dust and dirt may accumulate on the collector surface, for many installations, regular cleaning or maintenance mitigates this effect, making it negligible for analytical purposes.

6. The shading of the evacuated collector absorber plate is negligible.

Assuming negligible shading simplifies the analysis by disregarding the potential blocking of sunlight on the absorber plate by surrounding objects or structures. This assumption is valid in scenarios where the collector is properly positioned and oriented to receive maximum sunlight exposure throughout the day, minimizing shading effects.

7. The heat transfer processes are independent of time (steady state).

The steady-state conditions simplify the analysis by focusing on the long-term behavior of the system, where temperatures and heat transfer rates remain constant over time. This simplification allows us to solve for steady-state solutions, which are often easier to analyze and provide valuable insights into the system's performance under constant operating conditions.

Under the above assumptions, the thermal balance concerning with of outer absorber surface can be written as

$$\phi_a = \phi_d + \phi_u \qquad (18)$$

Where

ϕ_a : Is the absorbed heat flux in W , expressed as

$$\phi_a = \tau_c \alpha_a S_{ao} G \qquad (19)$$

S_{ao} : is the outer surface of the absorber in m^2 .

τ_c, α_a : Are the transmissivity and the absorptivity of cover and absorber respectively

G : Is the solar incident flux density in $W.m^{-2}$.

ϕ_u : Is the useful heat flux in W , given by

$$\phi_u = m^\bullet C \left(T_{fo} - T_{fi} \right) \qquad (20)$$

Where

$m^\bullet$: Is the mass flow of the working fluid in $Kg.s^{-1}$.

C : Is heat capacity of the working fluid in $J.Kg^{-1}.s^{-1}$.

T_{fi} : Is the inlet temperature of the working fluid in K .

T_{fo} : Is the outlet temperature of the working fluid in K .

We can alternatively express the elementary variation of the useful flux as follows

$$d\phi_u = d\phi_{a-a}^{cd} = d\phi_{a-f}^{cv} \qquad (21)$$

Where $d\phi_{a-a}^{cd}$ is the elementary conductive flux crossing the absorber and $d\phi_{a-f}^{cv}$ is the elementary convective flux exchanged between the absorber and the working fluid in W . They are defined as:

$$d\phi_{a-a}^{cd} = H_{a-a}^{cd}(T_{ao} - T_{ai}) \times \frac{dx}{L} \qquad (22)$$

Where H_{a-a}^{cd} is conductive heat coefficient in $W.K^{-1}$ which is expressed as

$$H_{a-a}^{cd} = \frac{2\pi L \lambda_a}{\ln \dfrac{r_{ao}}{r_{ai}}} \qquad (23)$$

Where λ_a is the thermal conductivity of the absorber in $W.m^{-1}.K^{-1}$ and L is the length of the absorber in m while r_{ai} and r_{ao} are the inner and outer radii of the absorber in m .

Whereas

$$d\phi_{a-f}^{cv} = H_{a-f}^{cv}(T_{ai} - T_f)\frac{dx}{L} \qquad (24)$$

Where T_{ai} and T_{ao} the temperatures of the inner and outer surfaces of the absorber in K and H_{a-f}^{cv} is the convective heat coefficient in $W.K^{-1}$ which given by

$$H_{a-f}^{cv} = h_{a-f} S_{ai} \qquad (25)$$

S_{ai} is the inner surface of the absorber in m^2 and h_{a-f} Is the heat convection coefficient between the absorber and the working fluid $W.m^{-2}.K^{-1}$, calculable using Nusselt correlations, listed in table 2 and λ_a is the thermal conductivity of the absorber.

Finally, the thermal efficiency of the evacuated solar collector can be expressed as the ratio of the useful flux to the absorbed flux as [3] [11].

$$\eta = \frac{m^{\bullet}C\left(T_{fo} - T_{fi}\right)}{\tau_c \alpha_a S_{ao} G} \qquad (26)$$

We can define the dissipated flux by means of the energy conservation law as

$$\phi_d = \phi_{a-c}^{rd} = \phi_{c-c}^{cd} = \phi_{c-e}^{rd} + \phi_{c-e}^{cv} \qquad (27)$$

This can easily allow to alternatively express the dissipated flux as

$$\phi_d = H_{gl}^{th} S_{ao}\left(T_{ao} - T_{ev}\right) \qquad (28)$$

Where ϕ_d is the dissipated flux in W and H_{gl}^{th} is the global heat coefficient in $W.m^{-2}..K^{-1}$ which is given by

$$H_{gl}^{th} = \frac{1}{\dfrac{1}{H_{a-c}^{rd}} + \dfrac{1}{H_{c-c}^{cd}} + \dfrac{1}{H_{c-e}^{rd} + H_{c-e}^{cv}}} \qquad (29)$$

While

$H_{a-c}^{rd}, H_{c-c}^{cd}, H_{c-e}^{rd}$ and H_{c-e}^{cv} are accordingly the radiative heat coefficient between the absorber and cover, the conductive heat coefficient through the cover , the radiative heat coefficient between the cover and environment and convective heat coefficient between the cover and environment in convective heat exchange in $W.K^{-1}$. They are defined as:

$$H_{a-c}^{rd} = \frac{\sigma\left(T_{ao}^2 + T_{ci}^2\right)\left(T_{ao} + T_{ci}\right)}{\dfrac{1}{\varepsilon_a} + \dfrac{1-\varepsilon_c}{\varepsilon_c}\left(\dfrac{r_{ao}}{r_{ci}}\right)} \qquad (30)$$

Where σ is the Stefan-Boltzmann constant in $W.K^{-4}.m^{-2}$, T_{ci} is the inner temperature of the cover in K, r_{ci} is the inner radius of the cover in m, ε_a and ε_c are the emissivities of the absorber and the cover respectively.

$$H_{c-e}^{rd} = \frac{S_{co}\sigma\varepsilon_c\left(T_{co}^4 - \varepsilon_e T_{ev}^4\right)}{S_{ao}\left(T_{co} - T_{ev}\right)} \qquad (31)$$

And

$$H_{c-c}^{cd} = \frac{2\pi L \lambda c}{S_{ao} \ln \dfrac{r_{co}}{r_{ci}}} \qquad (32)$$

And

$$H_{c-e}^{cv} = \frac{S_{co}}{S_{ao}}.h_{c-e} \qquad (33)$$

Where ϕ_{a-c}^{rd} , ϕ_{c-c}^{cd}, ϕ_{c-e}^{rd} and ϕ_{c-e}^{cv} depicted in equation (27) are correspondingly the radiative dissipated flux between the absorber and the cover in W , the conductive dissipated flux through the cover in W , the radiative dissipated flux between the cover and the environment, in W and the convective dissipated flux between the cover and the environment in W . They are defined in the following order as

$$\phi_{a-c}^{rd} = H_{a-c}^{rd} S_{ao} \left(T_{ao} - T_{ci} \right) \qquad (34)$$

And

$$\phi_{c-c}^{cd} = H_{c-c}^{cd} S_{ao} \left(T_{ci} - T_{co} \right) \qquad (35)$$

And

$$\phi_{c-e}^{cv} = H_{c-e}^{cv} S_{ao} \left(T_{co} - T_{ev} \right) \qquad (36)$$

And

$$\phi_{c-e}^{rd} = H_{a-e}^{rd} S_{ao} \left(T_{co} - T_{ev} \right) \qquad (37)$$

II.2.3 Determination of the working fluid temperature distribution along the absorber

We can perform a thermal balance by equalizing the elementary useful flux transmitted to working fluid through the absorber thickness by conduction and between the absorber and the working fluid by convection and inside the working fluid due to its temperature rising as. Therefore, the temperature distribution can be expressed as:

$$d\phi_u = d\phi_{a-a}^{cd} = d\phi_{a-f}^{cv} \Leftrightarrow m^\bullet C dT_f = H_{a-a}^{cd}\left(T_{ao} - T_{ai}\right) \times \frac{dx}{L} = H_{a-f}^{cv}\left(T_{ai} - T_f\right)\frac{dx}{L} \qquad (38)$$

Where

ϕ_{a-a}^{cd} and ϕ_{a-f}^{cv} are the conductive flux transmitted to the working fluid in W, and the convective flux transmitted to the working in W.

They are given by

$$\phi_{a-a}^{cd} = H_{a-a}^{cd} S_{ao}\left(T_{ao} - T_{ai}\right) \qquad (39)$$

And

$$\phi_{a-f}^{cv} = H_{a-f}^{cv} S_{ao}\left(T_{ai} - T_f\right) \qquad (40)$$

Now after, making some algebraic handling, we lead to

$$\frac{dT_f}{\phi_a + H_{gl}^{th}\left(T_{ev} - T_f\right)S_{ao}} = \frac{dx}{Lm^\bullet c\left(1 + \dfrac{H_{gl}^{th}}{H_{a-a}^{cd}} + \dfrac{H_{gl}^{th}}{H_{a-f}^{cv}}\right)} \qquad (41)$$

By integrating both sides of the above equation, we obtain

$$\int_{T_{fi}}^{T_f} \frac{dT_f}{\phi_a + H_{gl}^{th}\left(T_{ev} - T_f\right)S_{ao}} = \int_0^x \frac{dx}{Lm^\bullet c\left(1 + \dfrac{H_{gl}^{th}}{H_{a-a}} + \dfrac{H_{gl}^{th}}{H_{a-f}}\right)} \qquad (42)$$

Now, we make substitutions as

$$\frac{-1}{H_{gl}^{th}S_{ao}}\ln\left[\phi_a+H_{gl}^{th}\left(T_{ao}-T_f\right)S_{ao}\right]_{T_{fi}}^{T_f}=\left.\frac{x}{Lm^\bullet C\left(1+\dfrac{H_{gl}^{th}}{H_{a-a}}+\dfrac{H_{gl}^{th}}{H_{a-f}}\right)}\right|_0^x \qquad (43)$$

Which results in

$$\frac{T_f-T_{ev}-\dfrac{\phi_a}{H_{gl}^{th}S_{ao}}}{T_{fi}-T_{ev}-\dfrac{\phi_a}{H_{gl}^{th}S_{ao}}}=e^{\dfrac{-H_{gl}^{th}S_{ao}x}{Lm^\bullet C\left(1+\dfrac{H_{gl}^{th}}{H_{a-a}}+\dfrac{H_{gl}^{th}}{H_{a-f}}\right)}} \qquad (44)$$

Or

$$T_f=T_{ev}+\frac{\phi_a}{H_{gl}^{th}S_{ao}}+\left[T_{fi}-T_{ev}-\frac{\phi_a}{H_{gl}^{th}S_{ao}}\right]\times e^{\dfrac{-H_{gl}^{th}S_{ao}X}{Lm^\bullet C\left(1+\dfrac{H_{gl}^{th}}{H_{a-a}}+\dfrac{H_{gl}^{th}}{H_{a-f}}\right)}} \qquad (45)$$

The above equation represents the evolution of the working fluid temperature along the absorber. We can thus compute the outlet temperature T_{fo} at the end of the absorber $x=L$ as

$$T_{fo}=T_{ev}+\frac{\phi_a}{H_{gl}^{th}S_{ao}}+\left[T_{fi}-T_{ev}-\frac{\phi_a}{H_{gl}^{th}S_{ao}}\right]\times e^{\dfrac{-H_{gl}^{th}S_{ao}}{m^\bullet C\left(1+\dfrac{H_{gl}^{th}}{H_{a-a}}+\dfrac{H_{gl}^{th}}{H_{a-f}}\right)}} \qquad (46)$$

Combining equations (20) and (41), we can finally provide a new and very practical algebraic formula to the useful flux that extremely assists the numerical calculation the thermal performance of evacuated solar tube as

$$\phi_u=\frac{S_{ao}\left(T_{fi}-T_{ev}\right)H_{gl}^{th}-\phi_a}{H_{gl}^{th}S_{ao}}\left[1-e^{\dfrac{-H_{gl}^{th}S_{ao}}{m^\bullet C\left(1+\dfrac{H_{gl}^{th}}{H_{a-a}}+\dfrac{H_{gl}^{th}}{H_{a-f}}\right)}}\right] \qquad (47)$$

II.3 Computational procedures

We will now reformulate the present thermal problem into more convenient algebra for more efficient numerical computation. In other word, we will represent the conductive, convective and radiative exchanged heat concerning with the evacuated solar collector by a set of coupled and highly nonlinear equations by means the conservation of the thermal fluxes equations previously discussed as

The only unknowns here are the four temperatures T_{ai}, T_{ao}, T_{ci} and T_{co} which are computed iteratively in this work using a fixed-point method. The convergence of this fixed-point method is well discussed in [17][18][19]. However, the numerical solution of the problem still strongly depends of the values of the first guesses that should be taken very close to roots to ensure convergence of the method. Otherwise, the method would not be numerically stable and probably overflow. To avoid any numerical instability, the initial guesses to start the fixed-point iterative method have been selected using certain logical and physical considerations as follows

$$T_f < T_{ai} < T_{ao} > T_{ci} > T_{co} > T_{ev} \qquad (48)$$

And

$$\begin{aligned}
T_{ao} &= T_{ev} + \Delta T \\
T_{ai} &= T_{ev} + \frac{3\Delta T}{4} \\
T_{ci} &= T_{ev} + \frac{2\Delta T}{4} \\
T_{co} &= T_{ev} + \frac{\Delta T}{4}
\end{aligned} \qquad (49)$$

Where is ΔT a temperature shift.

We transform equations (27) and (28) into more suitable forms for numerical calculations as

$$T_{ci} = T_{ao} - \frac{\phi_d}{H_{a-c}^{rd} S_{ao}} \qquad (50)$$

And

$$T_{co} = T_{ci} - \frac{\phi_d}{H_{c-c}^{cd} S_{ao}} \qquad (51)$$

And

$$T_{co} = T_{ci} - \frac{\phi_d}{H_{c-c}^{cd} S_{ao}}$$ (52)

And

$$T_{ai} = T_{ao} - \frac{\phi_u}{H_{a-a}^{cd} S_{ao}}$$ (53)

The following flowchart summarizes all the numerical steps that have been used to solve the set of equations (50) , (51), (52) and (53) and therefore compute the values of the set of the temperatures T_{ai}, T_{ao}, T_{ci} and T_{co} which allows the evaluation of the entire thermal performances concerning with the present direct flow evacuated solar collector.
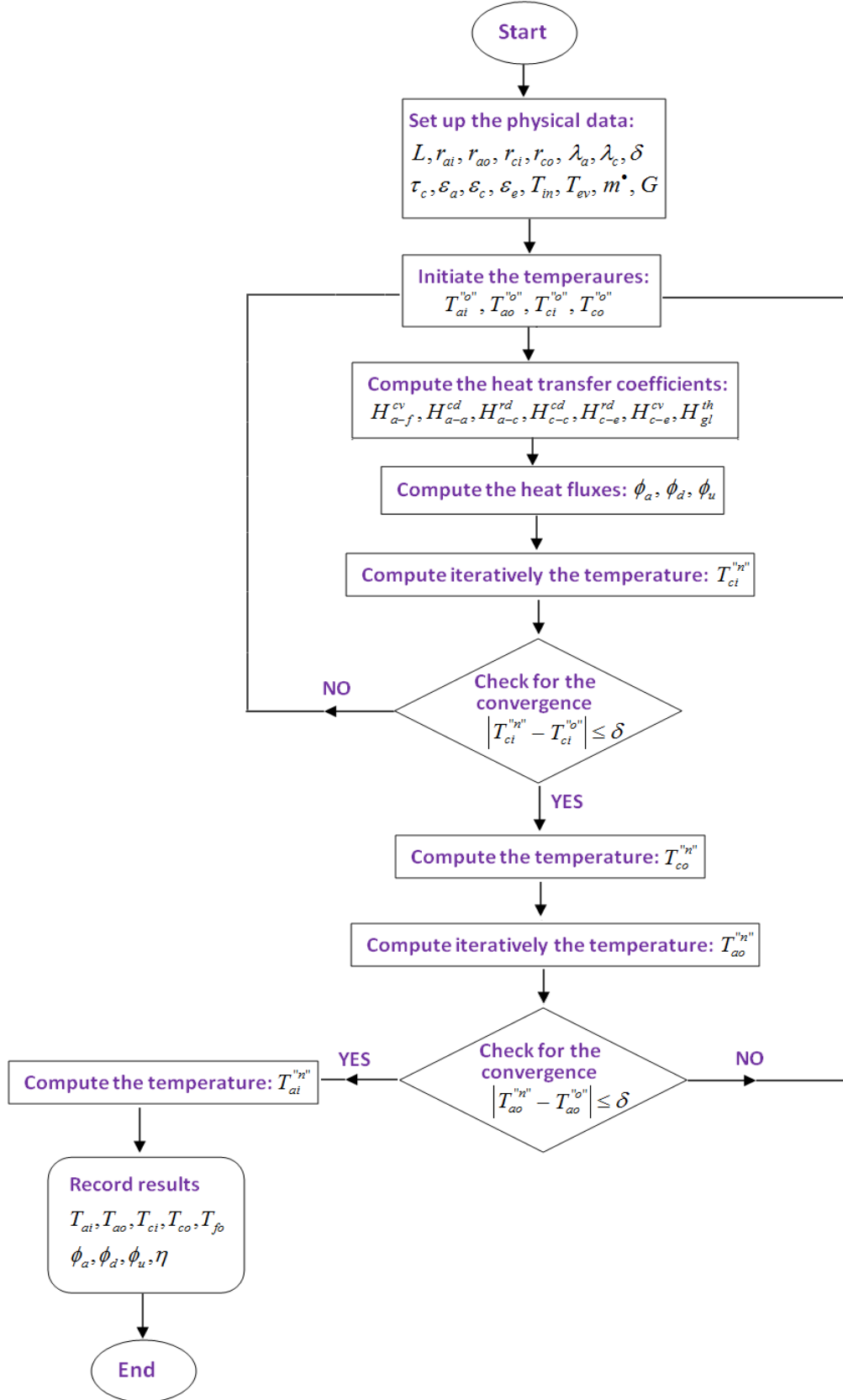
Figure 10: Computational flowchart for a direct flow evacuated solar collector thermal performances.

Chapter III
Results
and Discussion

Chapter III Results and Discussion

We will present in this chapter miscellaneous results concerning with a direct flow evacuated solar collector implemented by a FORTRAN code that mainly aims to compute the thermal performance of the solar device such as the efficiency, the useful heat flux, the dissipated heat flux and the outlet temperature using the fixed-point method for the physical data listed in the table below, table **8**.

Table 8 Lists of the number of physical parameters employed in the numerical simulation of the direct flow evacuated solar tube

Absorber length	0.6 m
Absorber inner radius	0.013m
Absorber outer radius	0.015 m
Absorber thermal conductivity	400 W.m^{-1}. K^{-1}
Cover length	0.6 m
Cover inner radius	0.03
Cover outer radius	0.04
Cover thermal conductivity	0.8 W.m^{-1}. K^{-1}
Inlet temperature	10 $^{\circ}$C
Environment temperature	10 $^{\circ}$C
Absorber emissivity	0.95
Cover emissivity	0.95
Environment emissivity	0.95
Mass flow	0.001 Kg. s^{-1}
Incident radiation flux density	400 W.m^{-2}

It should be mentioned that all the above physical parameters are maintained constant during the numerical computation until we vary each one of them separately to visualize its influence on the thermal performance of the solar device cited previously.

It must be also pointed out that the set of the governing equations (51), (52), (53) and (54) of the present direct flow evacuated solar tube are highly nonlinear that absolutely requires a very careful numerical treatment to provide satisfactory results. The Initial guesses to start the fixed-

point iterative method have been selected using a number of logical and physical considerations as follows

$$T_f < T_{ai} < T_{ao} > T_{ci} > T_{co} > T_{ev}$$
$$And$$
$$T_{ao} = T_{ev} + 20$$
$$T_{ai} = T_{ev} + 10$$
$$T_{ci} = T_{ev} + 15$$
$$T_{co} = T_{ev} + 5$$

As it is obviously shown that the set of the four unknown temperatures $T_{ai}, T_{ao}, T_{ci}, T_{co}$ are physically arranged according to their order of magnitude and they all are written in terms of the environment temperature T_{ev} that we can realistically set up at any season of the year. A feature that makes the initials guesses needed for the fixed-point method stay close to the roots of equations (48) and (49) and consequently avoid any kind of numerical instability overflow or underflow.

Figures 1, **2** and **3** correspondingly represent the number of iterations required for reaching the convergence of the fixed-point technique as a function of the mass flow, the absorber length and the incident radiation flux density for the physical values tabulated in the table **8**.
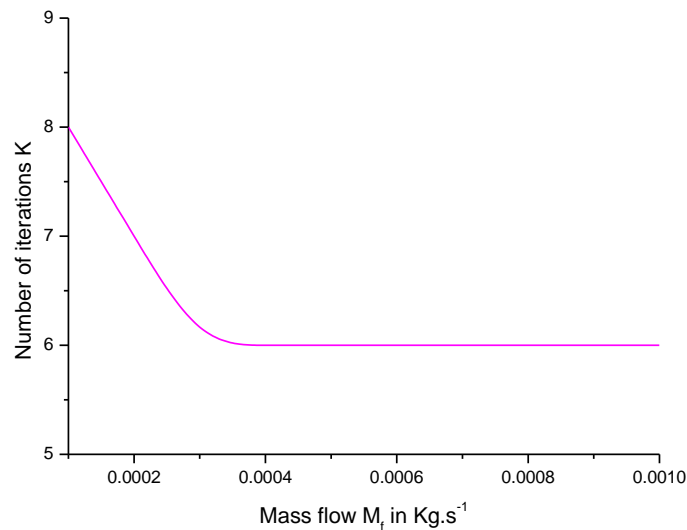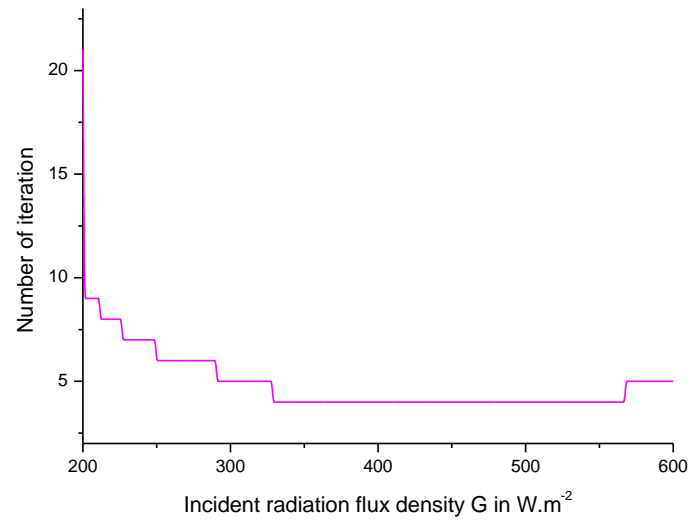

Figure 11: The number of iterations versus the mass flow

It is clearly shown that the speed of the convergence of the used method is very high in spite of the small value of the truncation tolerance $\varepsilon = 10^{-04}$ for the three curves which could also be seen as an excellent indicator of the robustness and the flexibility of the numerical method. It is also observed that the number iterations k smoothly decreases with the increase of the values the working fluid mass flow until it stagnates at about 6 as the mass flow keeps growing, **figure 11**.
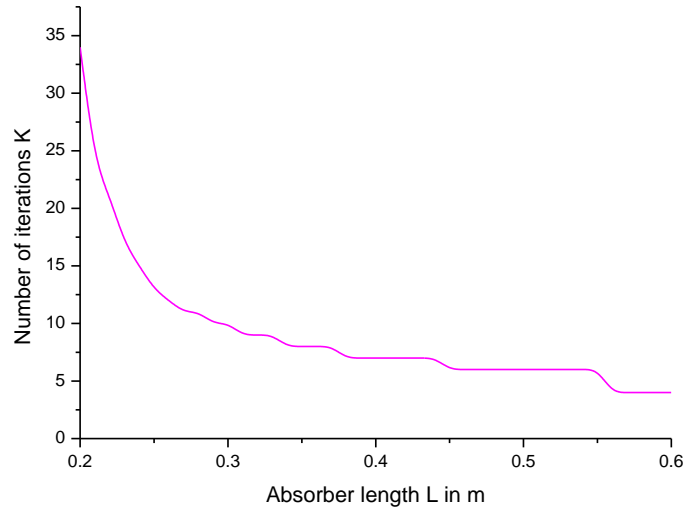

Figure 12: The number of iterations versus the absorber length

On the other hand, the number of iterations k constantly decreases with slight fluctuations as the absorber length rises, **figure 12** while it decreases and stagnates then increases with random fluctuations as the incident radiation flux density rises as it is shown in **figure 13**.

Figure 13: The number of iterations versus the incident radiation flux density
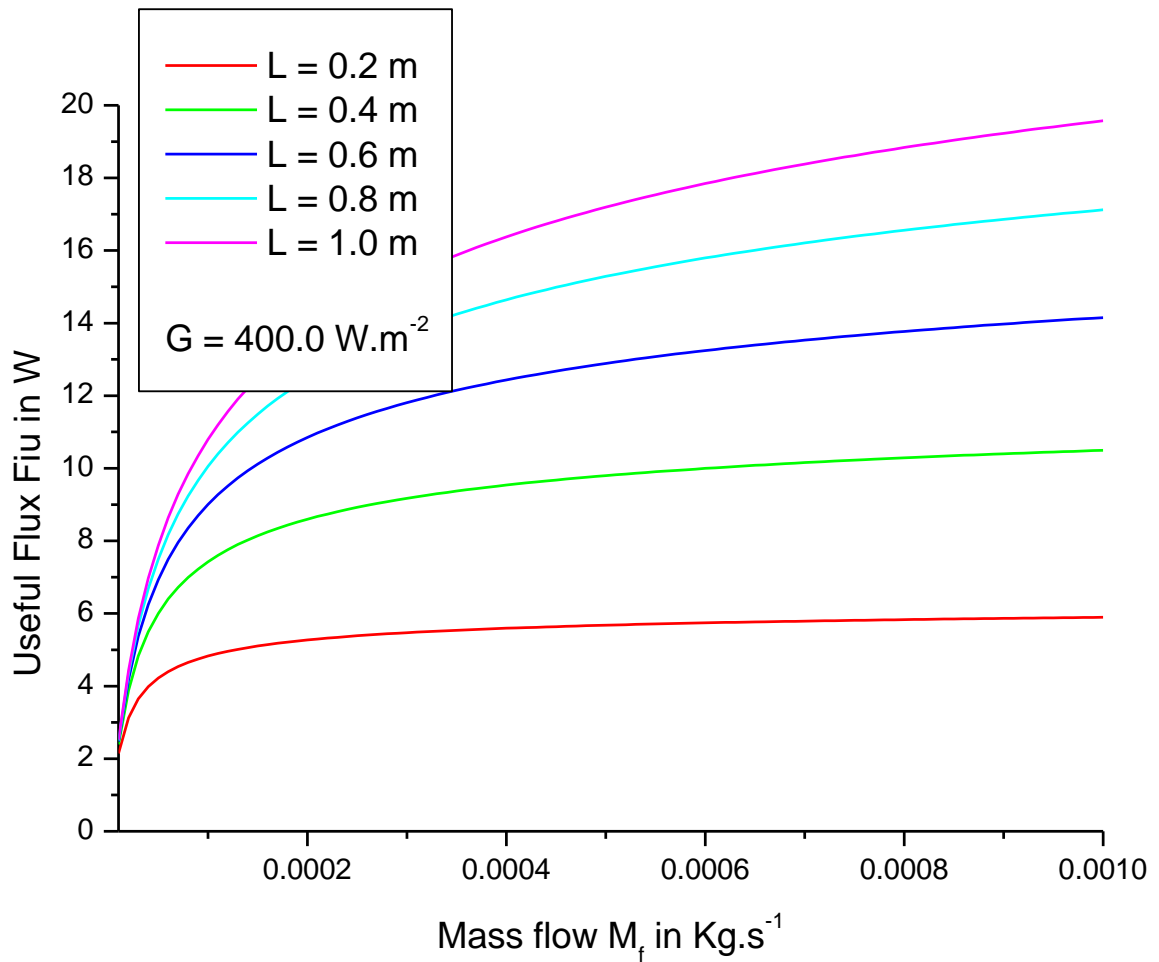
Results and Discussion:
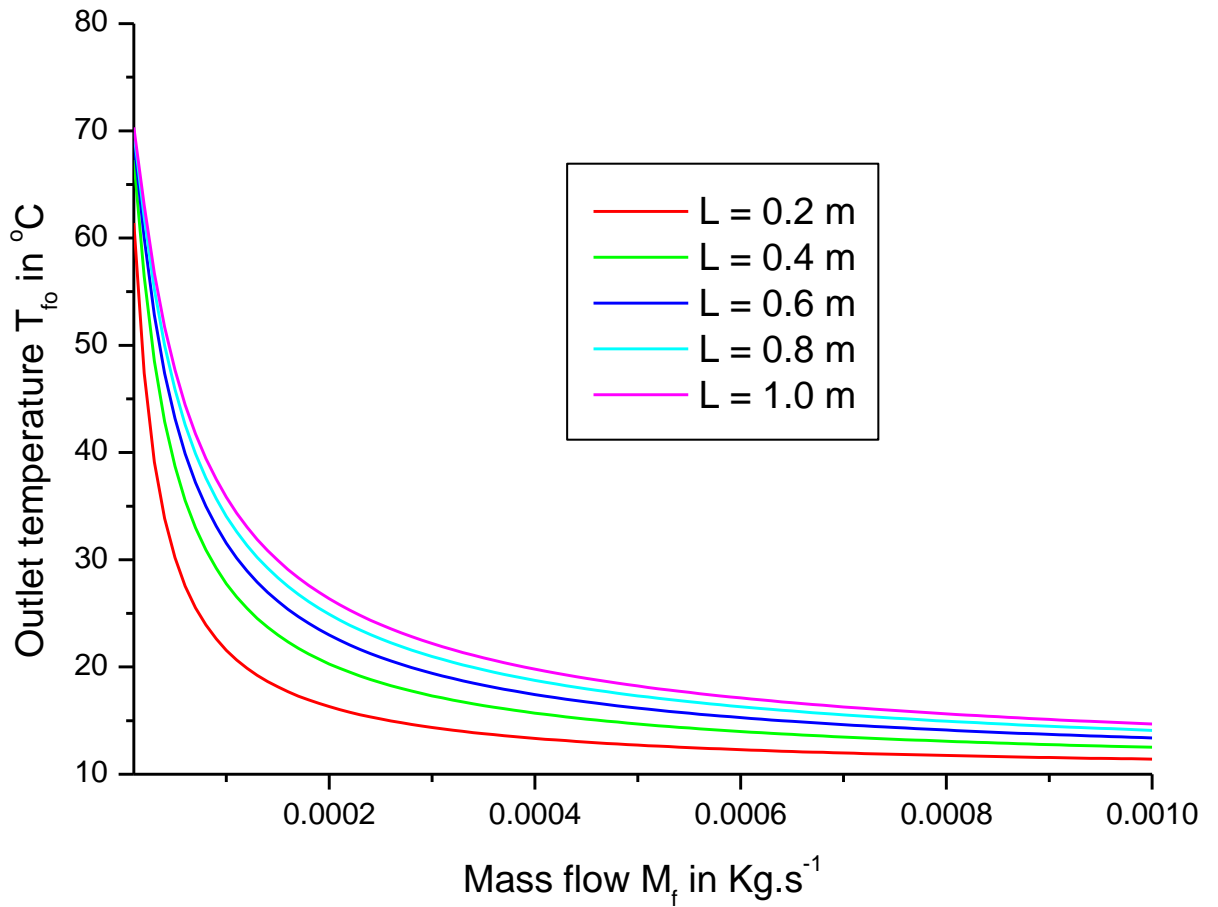
Figure 14: The outlet temperature versus the mass flow for different values of the absorber

The variation of the outlet temperature inside the absorber as a function of the working fluid mass flow for several values of the absorber length $L = 0.2, 0.4, 0.6, 0.8, 1.0m$ represented in **Figure 14.**

It is established that there is smooth reciprocal-like decrease of the outlet temperature as the mass flow of the working fluid increases which is significantly impacted by the change of the absorber length. The longer the absorber length is the higher the outlet temperature of the working fluid is.

Figure 15 provides the behavior of the useful flux inside the absorber as a function of the mass flow for various values of the absorber length $L = 0.2, 0.4, 0.6, 0.8, 1.0 m$. It is revealed that there is a smooth square-like grow of the useful flux as the mass flow of the working fluid increases. This incase is considerably improved by the rise of the length of the absorber.

Figure 15: The useful heat flux versus the mass flow for different values of the absorber length
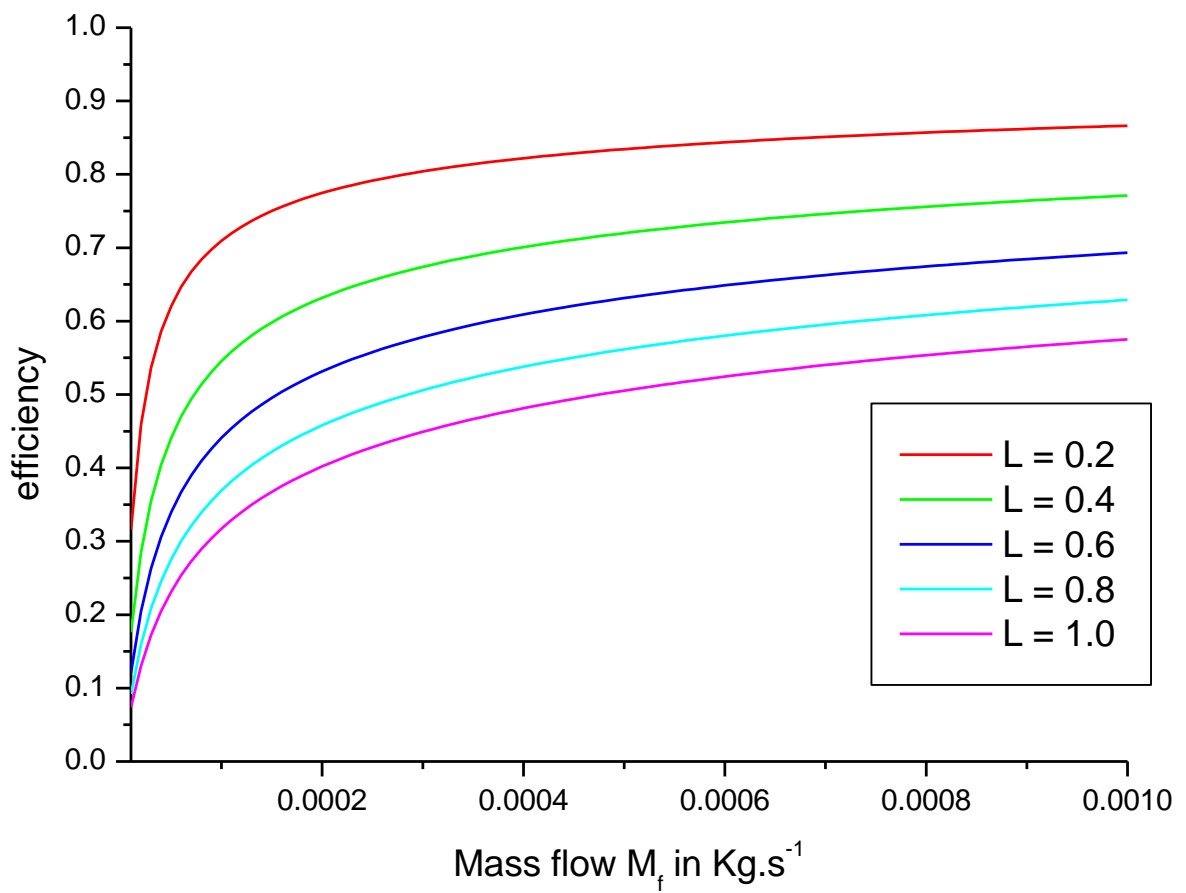
For different values of the absorber length $L = 0.2, 0.4, 0.6, 0.8, 1.0 m$, **figure 16** shows the conduct of the dissipated flux as a function of the mass flow. It is demonstrated that the magnitude of the dissipated heat flux smoothly drops as the absorber length rises.
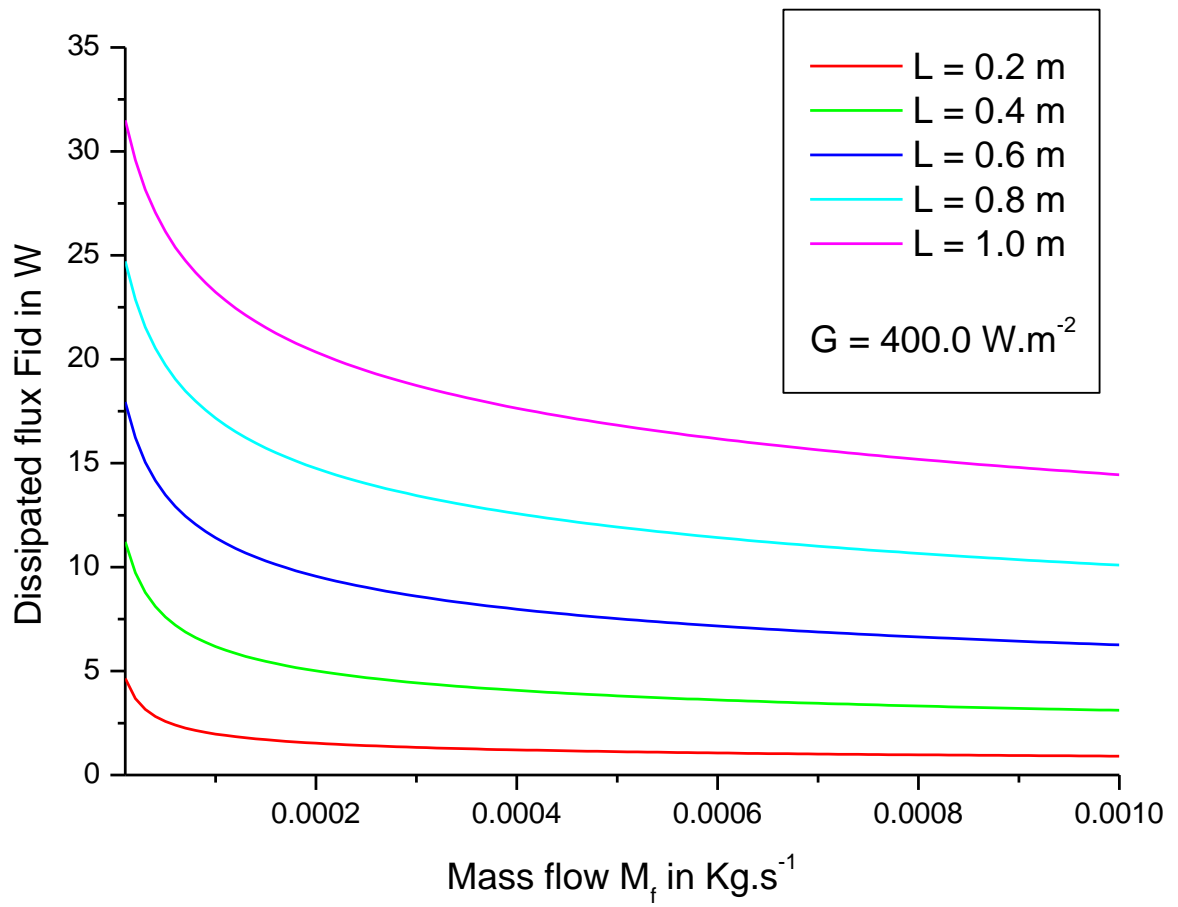
Figure 16: The dissipated heat flux versus the mass flow for different values of the absorber length

It is shown in **Figure 17** that the variation of the efficiency inside the absorber as a function of the mass flow for numerous values of the absorber length $L = 0.2, 0.4, 0.6, 0.8, 1.0m$. It is found that there is a steady development in the efficiency as the mass flow of the working fluid rises which is considerably influenced by the change of the absorber length. The smaller the absorber length is the higher the efficiency is.

Figure 17: The efficiency versus the mass flow for different values of the absorber length

Figure 18 displays data of the impact of the incident solar flux density on the outlet temperature as a function of the absorber length. For multiple intensities of the incident solar flux $G = 200, 300, 400, 500, 600 W.m^{-2}$ that typically corresponds a cold or mildly warm season, it is exhibited that there is proportional increase of the outlet temperature with the increase of the mass flow, where this increase can be positively impacted by the rise of the incident solar density.
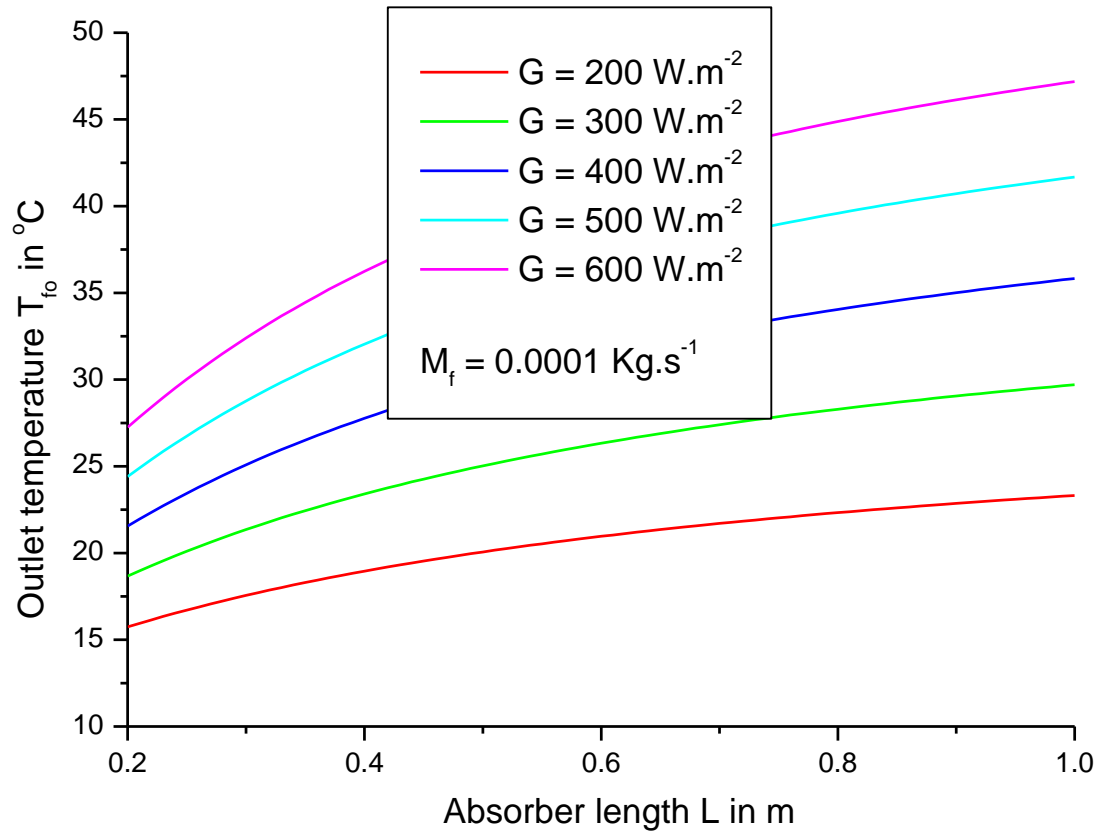
Figure 18: The outlet temperature versus the absorber length for different values of the incident radiation flux density

For several values of the incident radiation flux density $G = 200, 300, 400, 500, 600 \, in \, Wm^{-2}$,

figure 19 furnishes the thermal behavior of the useful heat flux as a function of the absorber length. It is numerically illustrated that there is a remarkable rise in the useful heat flux as the length of the absorber grows which is affected directly by the incident radiation flux density. The smaller the incident radiation flux density is the lower the useful heat flux is.
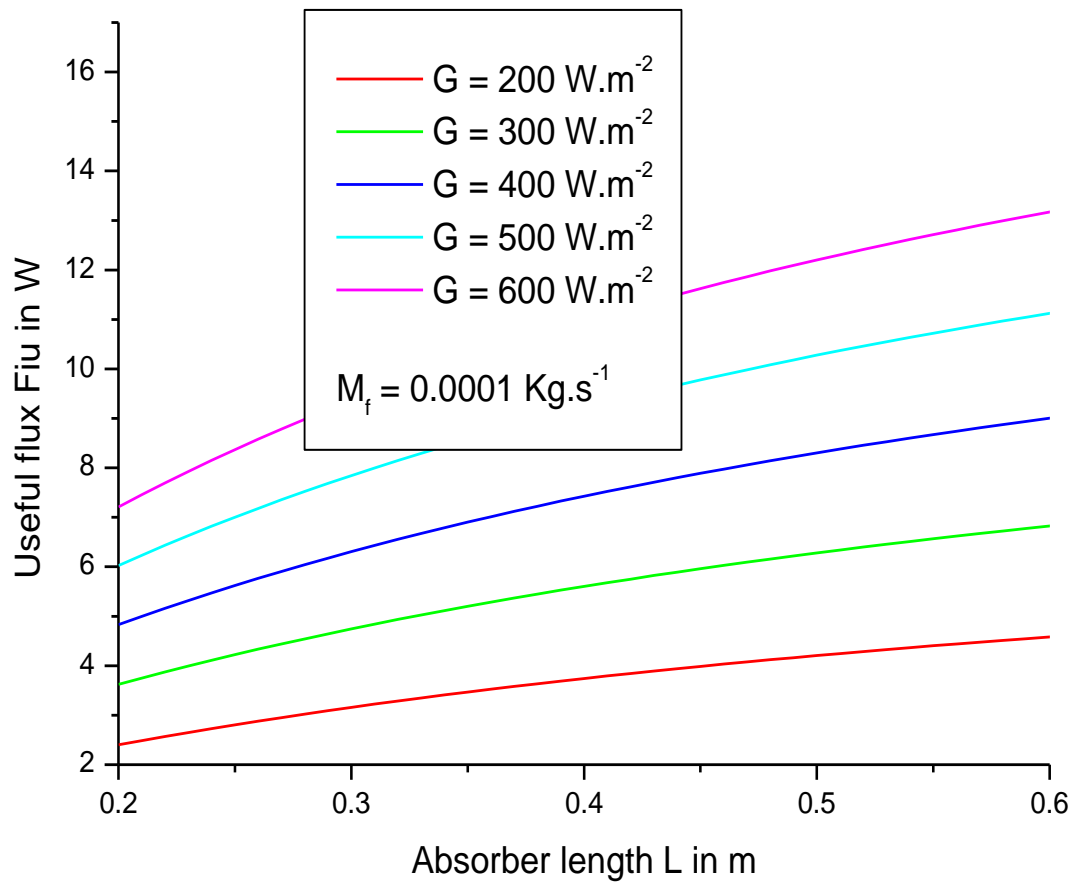
Figure 19: The useful heat flux versus the absorber length for different values of the incident radiation flux density

The variation of the dissipated heat flux as function of the absorber length depicted in **figure 20** for miscellaneous values of the incident radiation flux density $G = 200,300,400,500,600 \, in \, Wm^{-2}$ shows that there is an almost linear growing relationship between the dissipated heat flux and the absorber length which is certainly sensitive to the change of incident radiation flux density. The bigger the incident radiation flux density gets the higher the dissipated heat flux reaches.
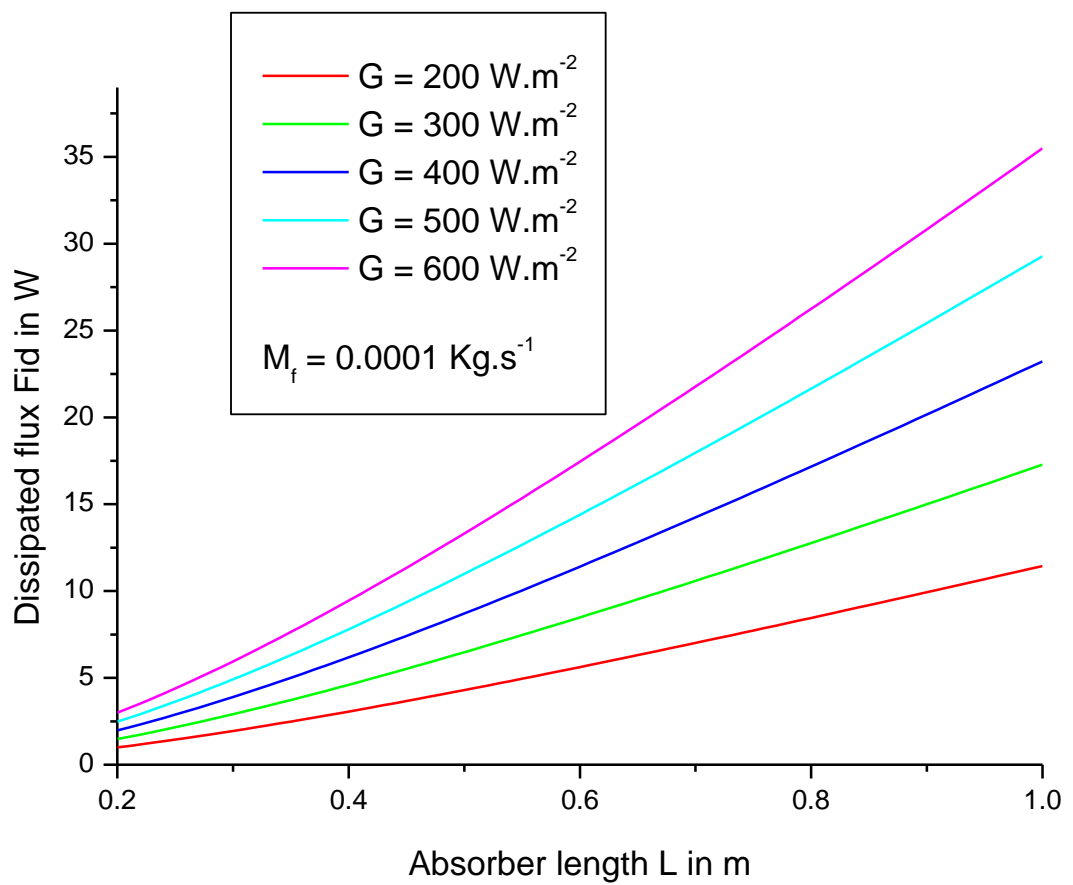
Figure 20: The dissipated heat flux versus the absorber length for different values of the incident radiation flux density
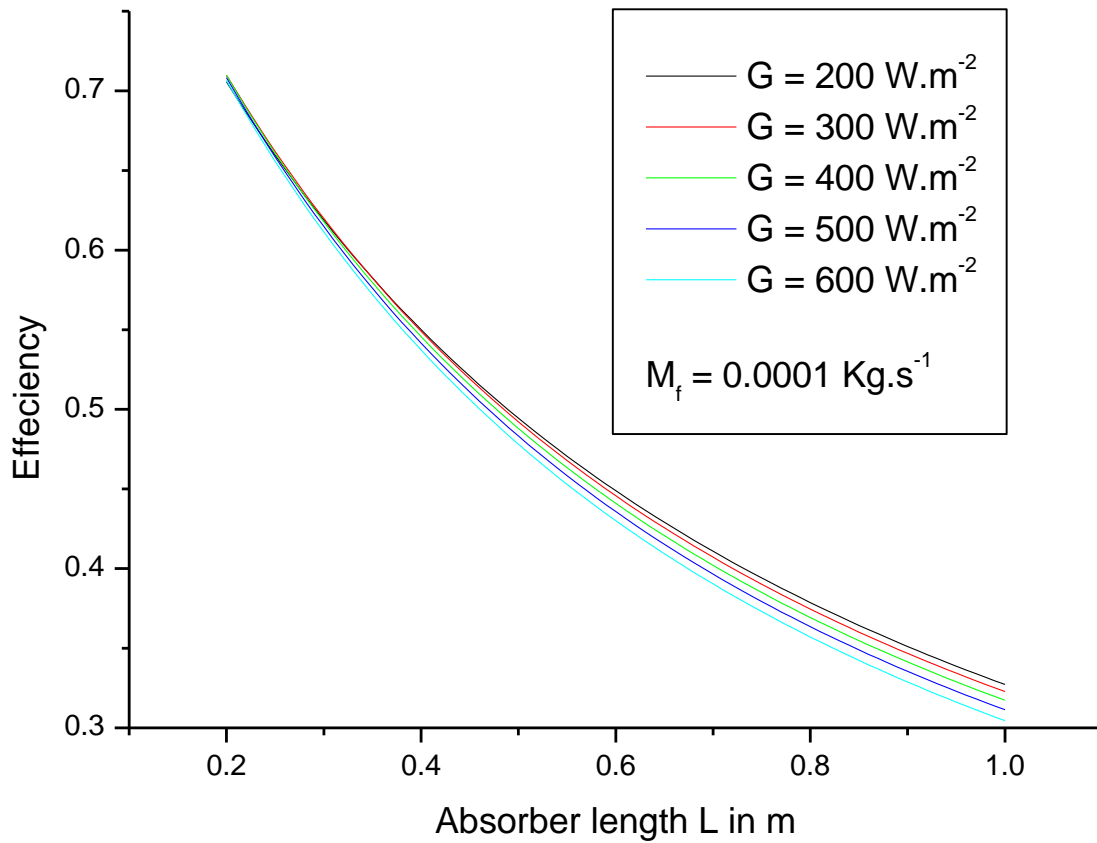
Figure 21: The efficiency versus the absorber length for different values of the incident radiation flux density

Figure 21 supplies important information   upon the connection between the efficiency and the absorber length for different values of the incident radiation flux density $G = 200,300,400,500,600 \, in \, Wm^{-2}$. It is clearly seen that there is a consistent decrease in the efficiency as the absorber gets longer which is notably affected by the value of the incident radiation flux density. The bigger the incident radiation flux density gets the lower the efficiency gets.
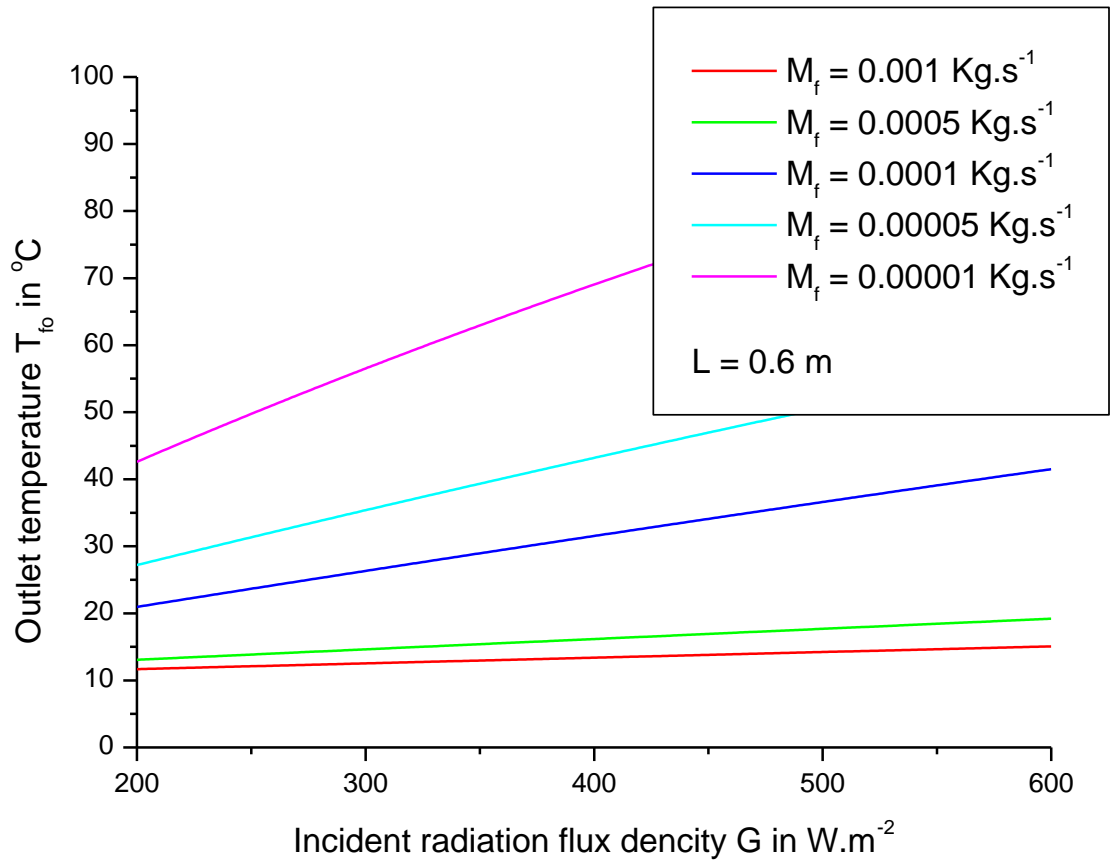
Figure 22: The outlet temperature versus the incident radiation flux density for different values of the mass flow

Figure 22 provides imperative information concerning the variation of the outlet temperature as a function of the incident radiation flux density for different values of the mass flow $M_f = 0.00001, 0.00005, 0.00.01, 0.0005, 0.001 Kg.s^{-1}$. It is evident that there is a notable increase in the outlet temperature as the incident radiation flux density increase which is impacted by the mass flow working fluid variation. The smaller the mass flow is the bigger the outlet temperature is.
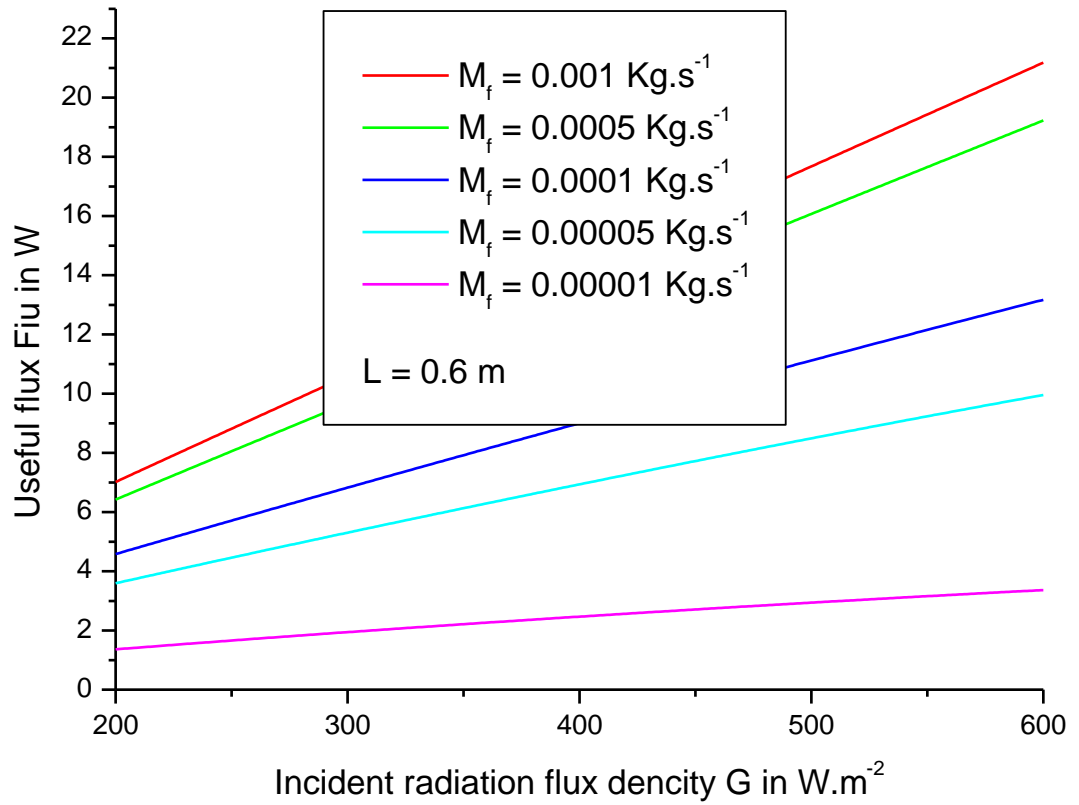
Figure 23: The useful heat flux versus the incident radiation flux density for different values of the mass flow

Figure 23 reveals vital thermal characteristics related to the behavior of the useful heat flux as a function of the incident radiation flux density for different values of the mass flow $M_f = 0.00001, 0.00005, 0.00.01, 0.0005, 0.001 Kg.s^{-1}$. It is clearly shown that there is an increase in the useful heat flux as the incident radiation flux density increase which is affected at the same time by the mass flow working fluid change. On other words, the bigger the mass flow is the bigger the useful heat flux is.
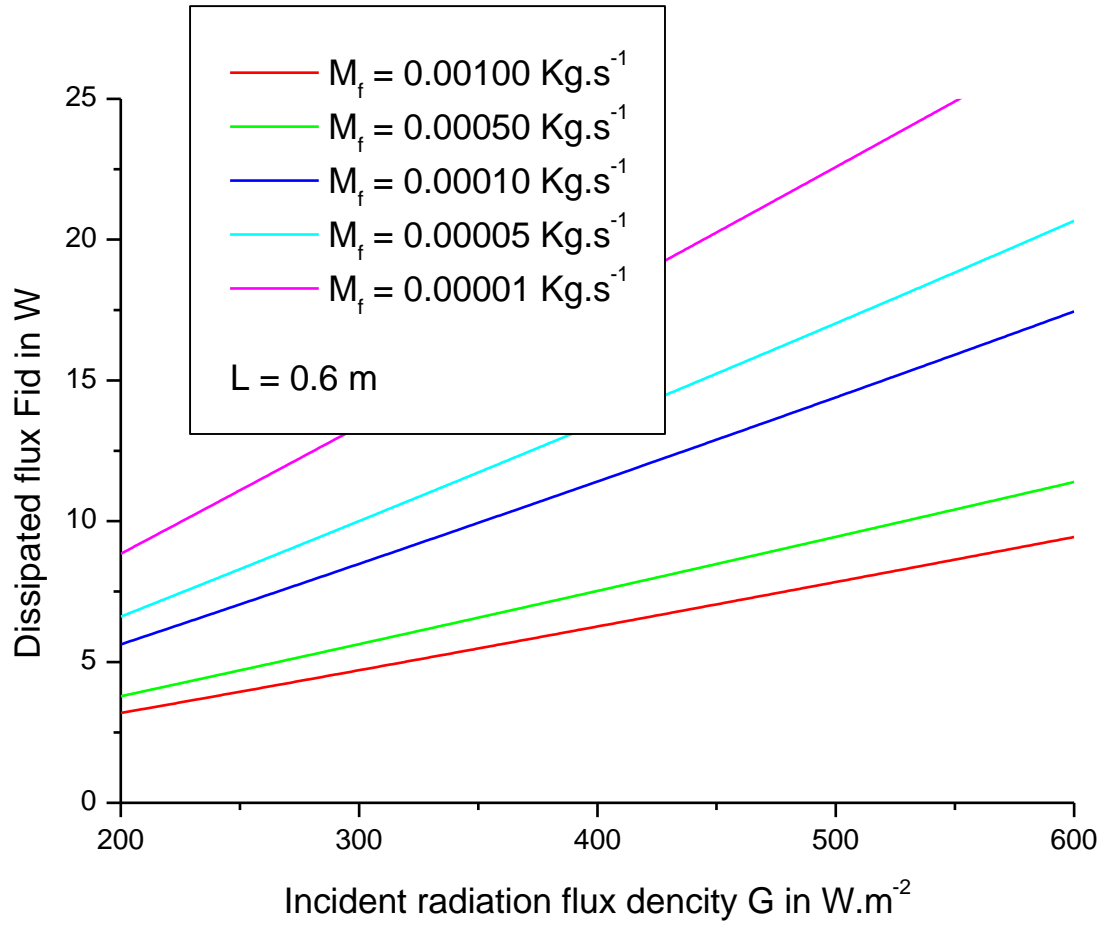
Figure 24: The dissipated heat flux versus the incident radiation flux density for different values of the mass flow

Figure 24 exhibits central features of the correlation between the useful heat flux and the incident radiation flux density for different values of the mass flow $M_f = 0.00001, 0.00005, 0.00.01, 0.0005, 0.001 Kg.s^{-1}$. It is visualized that there is a remarkable development in the useful heat flux as the incident radiation flux density increases which is also influenced by the mass flow working fluid values. The lesser the mass flow is the higher the useful heat flux is.
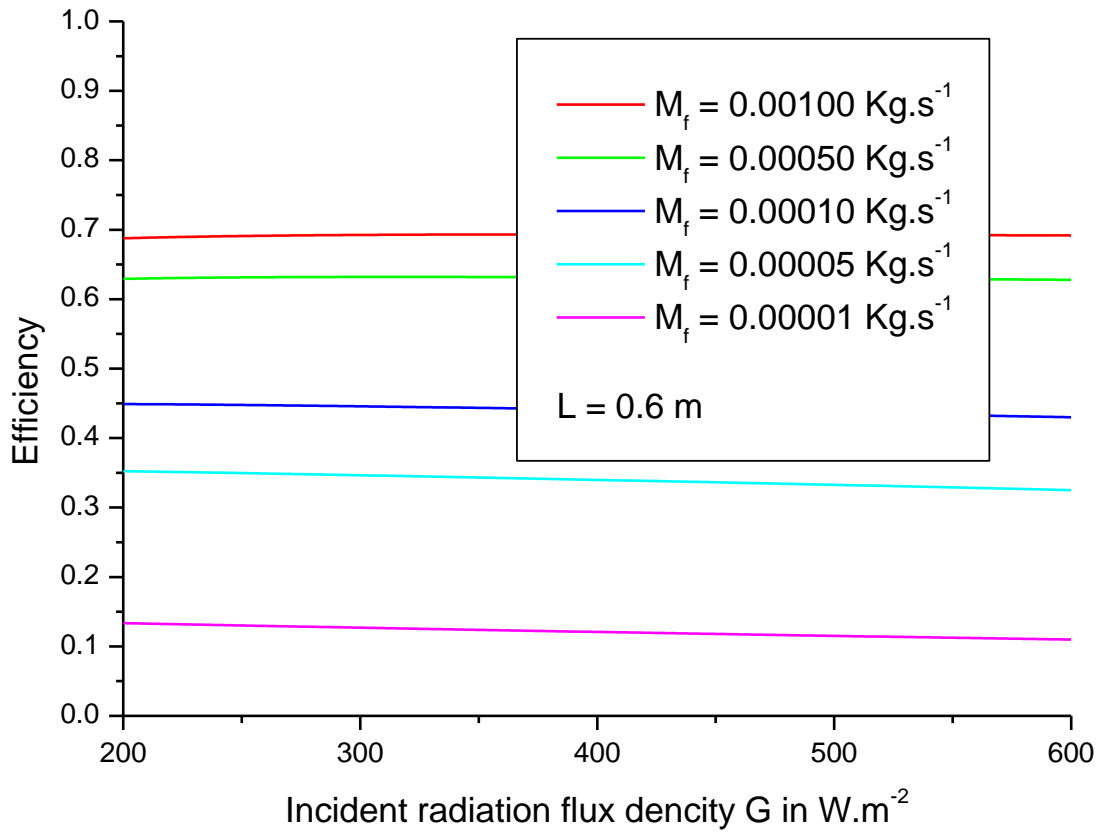
Figure 25: The efficiency versus the incident radiation flux density for different values of the mass flow

Figure 25 The variation of the efficiency of an evacuated solar tube as a function of the incident radiation flux density represented in (Fig. 18), for different values of the working fluid mass flow $M_f = 0.00001, 0.00005, 0.00.01, 0.0005, 0.001 Kg.s^{-1}$. It is observed that the efficiency is slightly affected by the change in the mass flow and shows flat horizontal curves as the incident solar flux grows.

The present study is entirely devoted to the solution generation and their thermal analysis where many thermal performances of the evacuated solar tube which are the efficiency, the outlet temperature of the working fluid, as well as the useful and the dissipated heat fluxes have been undertaken in great detail. Results have evidently shown the thermal response of each one of these thermal performances as functions of different physical data, which are the absorber length, the working fluid mass flow, and the incident solar flux density. It has also

been demonstrated that the fixed-point method is not only powerful but also flexible and speedy to handle this kind of complex thermal problem.

Conclusion:

The present chapter was entirely devoted to the solution generation and their thermal analysis where many thermal performances of the evacuated solar tube which are the efficiency, the outlet temperature of the working fluid, as well as the useful and the dissipated heat fluxes have been undertaken in great detail. Results have evidently shown the thermal response of each one of these thermal performances as functions of different physical data which are the absorber length, the working fluid mass flow, and the incident solar flux density. It has also been demonstrated that the fixed-point method is not only powerful but also flexible and speedy to handle this kind of complex thermal problem.

General Conclusion

General Conclusion:

In summary, this work delves into the realm of advancing the thermal design and optimizing the performance of direct-flow evacuated solar collectors, a highly effective solution for converting solar energy into thermal energy efficiently, particularly during winter when meteorological conditions are at their harshest.

By meticulously processing geometrical, physical, and meteorological data, this research

rigorously examines critical parameters, including solar incident energy, absorber length, and mass flow. These parameters hold the key to unlocking the thermal performance of the direct flow evacuated solar tubes, encompassing factors such as efficiency, useful heat flux, dissipated heat flux, and outlet temperature, all elegantly visualized through a series of graphic curves.

Notably, it has been observed that as the absorber length increases, there is a consistent decrease in efficiency, accompanied by changes in other key performance metrics such as useful heat flux, dissipated heat flux, and outlet temperature. This relationship underscores the critical importance of carefully selecting the absorber length to achieve optimal performance in direct-flow evacuated solar collectors.

Furthermore, the investigation revealed intriguing insights into the interplay between mass flow rate and system efficiency. It was found that variations in mass flow rate have a discernible effect on the efficiency of the collectors, with higher mass flow rates leading to increased efficiency. This correlation highlights the significance of fluid dynamics in dictating the overall performance of the system and underscores the importance of optimizing mass flow rates for enhanced efficiency.

Moreover, the influence of incident radiation flux density on system performance cannot be

overstated. The analysis demonstrated a direct correlation between incident radiation flux density and outlet temperature, with higher flux densities resulting in elevated outlet temperatures. This relationship underscores the importance of harnessing solar energy effectively, especially in regions with high solar irradiance, to maximize thermal energy conversion efficiency.

In essence, this study not only expands the frontiers of thermal design but also provides a

stepping-stone for a more sustainable future, where the efficient harnessing of solar energy holds immense promise. By embracing advancements such as direct-flow evacuated solar collectors, we inch closer to a world where renewable energy becomes the cornerstone of our energy infrastructure, ensuring a brighter and more sustainable tomorrow.

References

References

[1] Bergman, T. L., Lavine, A. S., Incropera, F. P., & DeWitt, D. P. (2011). *Introduction to Heat Transfer*. John Wiley & Sons.

[2] Bergman, T. L., Incropera, F. P., DeWitt, D. P., & Lavine, A. S. (2011). *Fundamentals of Heat and Mass Transfer*. John Wiley & Sons.

[3] Jannot, Y., & Degiovanni, A. (2018). *Thermal Properties Measurement of Materials*. John Wiley & Sons.

[4] Mills, A., & Coimbra, C. F. M. (201000). *Basic Heat and Mass Transfer*.

[5] Kreith, F., Manglik, R. M., & Bohn, M. S. (2011). *Principles of Heat Transfer seventh Edition,* Cengage Learning.

[6] Lienhard, J. H. (2019). *A Heat Transfer Textbook: Fifth Edition*. Courier Dover Publications.

 [**7**] Amir Akbari et al. (2019). *Natural Convection from the Outside Surface of an Inclined Cylinder in Pure Liquids at Low Flux,* American Chemistry Society, No 4, Pp 7038-7046.

[8] Jeong-Hwan Heo and Bum-Jin Chung**. (**2012**)**. *Natural convection heat transfer on the outer surface of inclined cylinders,* Chemical Engineering Science, No 73, Pp 366-372**.** 2012.

[9] Akram W. Ezzat and Hassan W. Zghaer. (2013) *Forced Convection Heat Transfer Around Heated Inclined Cylinder,* International Journal of Computer Applications, No 8, Pp 0975-8887.

[10] Hablanian, H. J. (1998). *Vacuum Science and Technology: Fundamentals and Applications*. CRC Press.

[11] Duffie, J. A., & Beckman, W. A. (2013). *Solar Engineering of Thermal Processes*. John

Wiley & Sons.

[12] Bergman, T. L., DeWitt, D. P., Incropera, F. P., & Lavine, A. S. (2017). *Incropera's*

Principles of Heat and Mass Transfer.

[13] ENGINEERING SBI4U Course, *Radiation Heat Transfer*, chapter 12.

https://www.coursehero.com/file/77767849/cen58933-ch12pdf/ 9/9/20029:48 AM

[14] Chandraprabu, V., & Solomon, G. (2015). *Evacuated Tube Solar Collectors: A Review.*
International Journal of Scientific Engineering and Research (IJSER), 6(12), Pp 138 - 141.

[15] V.S. Kaluba; P. Ferrer (2016). *A modal for a Hot Mirror Coating Solar Parabolic trough
recievers.* Journal of Renewable and Sustainable Energy 8, 053703.

[16] Hablanian, H. J. (1998). *Vacuum Science and Technology: Fundamentals and
Applications.* CRC Press.

[17] Rheinboldt, W. C. (1998). *Methods for Solving Systems of Nonlinear Equations: Second*

Edition. SIAM.

[18] Burden, R. L., & Faires, J. D. (2010). *Numerical Analysis*. Cengage Learning.

[19] Hoffman, J. D., & Frankel, S. (2001). *Numerical Methods for Engineers and Scientists,*

Second Edition. CRC Press.

[20] Kalogirou, S. A. (2009). *Solar Energy Engineering: Processes and Systems*. Academic

Press.

Appendix

Appendix

1 Thermal proprieties of the air

The following experimental correlations of thermal properties of the air are valid for the range of temperature $0^{\circ}C - 100^{\circ}C$.

$$\rho = \frac{353}{T + 273} \quad in \; Kg.m^{-3}$$

$$C = 1008 \quad in \; J.Kg.^{-1}K^{-1}$$

$$\lambda = 7.75 \times 10^{-5}T + 0.0242 \quad in \; W.m.^{-1}K^{-1}$$

$$\mu = 10^{-5} \times (0.0046T + 1.7176) \quad in \; Pa.S$$

$$\alpha = 10^{-5} \times (0.0146T + 1.8343) \quad in \; m^{-2}.S^{-1}$$

$$pr = -2.54 \times 10^{-4}T + 0.7147$$

$$\beta \approx \frac{1}{T} \quad in \; K^{-1}$$

2 Thermal proprieties of water

The following experimental correlations of thermal properties of the water are valid for the range of temperature $0^{\circ}C - 100^{\circ}C$.

$$\rho = -0.00380T^{2} - 0.0505T + 1002.6 \quad in \; Kg.m^{-3}$$

$$C = 4180 \quad in \; J.Kg.^{-1}K^{-1}$$

$$\lambda = -9.87 \times 10^{-6} \times T^{2} + 2.238 \times 10^{-3} \times T + 0.5536 \quad in \; W.m.^{-1}K^{-1}$$

$$\mu = 10^{-4} \times (0.00200T^{2} + 0.3389T + 17.199) \quad in \; Pa.S$$

$$\alpha = 10^{-7} \times (-0.00360T + 1.340) \quad in \; m^{-2}.S^{-1}$$

$$Pr = 1.557 \times 10^{-3}T - 0.0261T + 12.501$$

$$\frac{g\beta\rho^{2}C}{\mu\lambda} = (0.0105T^{2} + 0.477T + 0.0363) \times 10^{9} \quad in \; K^{-1}.m^{-3}$$

3 Signification of certain dimensionless numbers

name	symbol	Formula	Physical signification
Biot number	B_i	$B_i = \dfrac{hL}{\lambda}$	Dimensionless number which approximates the ratio of the buoyancy to viscous forces acting on a fluid.
Grashof number	Gr	$Gr = \dfrac{g\beta(T_s - T_\infty)L^3}{v^2}$	Dimensionless number which approximates the ratio of the buoyancy to viscous forces acting on a fluid.
Nusselt number	Nu	$Nu = \dfrac{hd}{k}$	Is the ratio of convective to conductive heat transfer across a boundary.
Prandtl number	Pr	$Pr = \dfrac{v}{\alpha} = \dfrac{c_p\mu}{k}$	Is signifies the ratio of momentum diffusivity to thermal diffusivity.
Rayleigh number	Ra	$Ra = \dfrac{g\beta}{v\alpha}(T_s - T_\infty)L^3$	Is a dimensionless term used in the calculation of natural convection.
Reynolds number	Re	$Re = \dfrac{VL\rho}{\mu} = \dfrac{VL}{v}$	A dimensionless quantity that helps predict fluid flow patterns in different situations by measuring the ratio between inertial and viscous forces.
Fourier number	F_o	$F_o = \dfrac{\alpha t}{L^2}$	A dimensionless group which arises naturally from the nondimensionalization of the conduction equation.

4 The vacuum between the tubes

In evacuated solar tubes, sunlight is primarily absorbed rather than reflected. The inner metal tube of the evacuated solar tube is coated with a selective coating, which is designed to have high solar absorbance. This means that when sunlight enters the tube, the coating absorbs a significant portion of the solar radiation.

The selective coating is typically dark in color, as darker surfaces tend to absorb more light. When the sunlight strikes the selective coating, the photons of the light are absorbed, and their energy is converted into heat. This heat is then transferred to the fluid flowing through the tube.

The vacuum between the tubes in evacuated solar tubes serves two main purposes:

1. Insulation: The vacuum acts as an insulating layer, reducing heat loss from the inner tube to the outer tube and the surrounding environment. Without the vacuum, heat

could be conducted or convected from the inner tube to the outer tube, resulting in energy loss and reduced efficiency. The vacuum helps maintain higher temperatures within the inner tube, enhancing the overall thermal efficiency of the system.

2. Minimizing Convection: Convection is the transfer of heat through the movement of fluids or gases. By creating a vacuum, there is no air or gas to transfer heat through convection. This reduces convective heat loss, allowing more of the absorbed solar energy to be retained within the inner tube.

The combination of the selective coating on the inner tube, which absorbs sunlight, and the vacuum insulation between the tubes, which minimizes heat loss, helps maximize the efficiency of evacuated solar tubes in converting sunlight into thermal energy.

5 Fixed point method

The fixed point method is an iterative numerical technique used to solve equations by transforming them into fixed point equations. It is commonly used to find the roots of nonlinear equations.

The basic idea behind the fixed point method is to rewrite the original equation in the form of a fixed point equation, where the solution is expressed as a function of the previous approximation. The iterative process then generates a sequence of approximations that hopefully converge to the desired solution.

Here's a simplified overview of the fixed point method:

1. Start with an initial guess for the solution to the equation.

2. Rearrange the original equation to obtain an equivalent fixed point equation of the form x = g(x), where g(x) is a function.

3. Apply the iterative formula: x(n+1) = g(x(n)), where x(n) is the nth approximation and x(n+1) is the (n+1)th approximation.

4. Repeat the iteration process until convergence is achieved, which typically occurs when the difference between consecutive approximations falls below a specified tolerance level.

5. The final approximation obtained after convergence is considered as the solution to the equation.

It's important to note that the convergence of the fixed point method depends on the choice of the function g(x). The function must satisfy certain conditions, such as being continuous and having a derivative within a specified range, for convergence to occur.

6 The Code

```fortran
Program Vaccum

implicit none

integer::K

doubleprecision::Tai,Tao,taon,Tci,Tcin,Tco,Tev,Tfi,Tfo,DFT,Tol

doubleprecision::L,rai,rao,rci,rco,Sai,Sao,Sci,Sco

doubleprecision::Haa_cd,Haf_cv,Hac_rd,Hcc_cd,Hce_ra,Hce_cv,Hgl_th

doubleprecision::Faa_cd,Fac_rd,Fcc_cd,Fce_ra,Fce_cv

doubleprecision::Fia,Fiu,Fid

doubleprecision::Ka,Kc,Hf,He,Cf,Ce,Mf

doubleprecision::T_c,E_c,E_a,E_e,Sg

doubleprecision::G,Pi

!doubleprecision::Xmn,Xmx,DX

open(1,file='data.txt')

!Costant of Stefan-Boltzan

Sg    = 5.67E-08

!Compute Pi vlaue

Pi    = 4.0*atan(1.0)

!Truncation Ttolerance

TOl   = 1.00E-05

!Set up meteorogical data

Tev   = 10.0

Tfi   = 10.0

G     = 400.0

!Set up thermal data

Cf    = 4180.0

Ce    = 1002.0
```

```
Ka    = 400.0

Kc    = 0.8

He    = 10.0

Hf    = 10.0

Mf    = 0.0001
```

!Set up optical data

```
T_c   = 0.95

E_c   = 0.95

E_a   = 0.95

E_e   = 0.95
```

!Set up geometrical data

```
L     = 0.6

rco   = 0.04

rci   = rco-0.01

rao   = 0.02

rai   = rao-0.002
```

!Initiate the temperatures

```
Tai   = Tev+10.0

Tao   = Tev+15.0

Tci   = Tev+10.0

Tco   = Tev+05.0
```

!Compute the outer and outer surfaces of cover and absorber

```
Sco   = 2.0*Pi*rco*L

Sci   = 2.0*Pi*rci*L

Sao   = 2.0*Pi*rao*L

Sai   = 2.0*Pi*rai*L
```

!Compute the absorbed flux

Fia   = T_c*E_a*Sao*G

!Compute the conductive Cover heat tranfer coefficient

Hcc_cd = 2.0*Pi*L*Kc/(Sao*dlog(rco/rci))

!Compute the conductive Absorber heat tranfer coefficient

Haa_cd = 2.0*Pi*L*Ka/(Sao*dlog(rao/rai))

!Infinite loop "do 10" for computing iteratively the right temperature Tao

do 10

!count the number of iterations

K   = K+1

!Compute the convective Cover-Environment heat tranfer coefficient

Hce_cv = Sco*He/Sao

!Compute the radiative Absorber-Cover heat tranfer coefficient

Hac_rd =
Sg*((Tao+273.0)**2.0+(Tci+273.0)**2.0)*(Tao+273.0+Tci+273.0)/(1.0/E_a+((1.0-
E_c)/E_c)*(rao/rci))

!Compute the radiative Cover-Environment heat tranfer coefficient

Hce_ra = Sco*Sg*E_c*((Tco+273.0)**4.0-E_e*(Tev+273.0)**4.0)/(Sao*(Tco-Tev))

!Compute the global heat tranfer dissipation coefficient

Hgl_th = 1.0/(1.0/Hac_rd+1.0/Hcc_cd+1.0/(Hce_ra+Hce_cv))

!Compute the dissipated heat flux

Fid   = Sao *Hgl_th*(Tao-Tev)

!Infinite loop "do 20" for computing iteratively the right temperature Tci

do 20

Tcin   = Tao-
Fid/(Sao*Sg*((Tao+273.0)**2.0+(Tci+273.0)**2.0)*(Tao+273.0+Tci+273.0)/(1.0/E_a+((1.0
-E_c)/E_c)*(rao/rci)))

!Compute the temperature difference between the new and old values

DFT   = dabs(Tcin-Tci)

!Check for the convergence

```fortran
      if(DFT<= Tol) exit

      Tci    = Tcin

20    continue

      !The new temperature Tci

      Tci    = Tcin

      !The new temperature Tco

      Tco    = Tci-Fid/(Sao*Hcc_cd)

      !Compute the convective Absorber-Fluid heat tranfer coefficient

      Haf_cv = Sai*Hf/Sao

      !Compute the useful heat flux

      Fiu    = Mf*Cf*(Fia-Sao*Hgl_th*(Tfi-Tev))*(1.0-dexp(-
     Sao*Hgl_th/(Mf*Cf*(1.0+Hgl_th/Haa_cd+Hgl_th/Haf_cv))))/(Sao*Hgl_th)

      !Compute the outlet Temperature

      !Tfo    = Tev+Fia/(Sao*Hgl_th)-(Fia-Sao*Hgl_th*(Tfi-Tev))*exp(-
     Sao*Hgl_th/(Mf*Cf*(1.0+Hgl_th/Haa_cd+Hgl_th/Haf_cv)))/(Sao*Hgl_th)

      Tfo    = Tfi+Fiu/(Mf*Cf)

      !Compute the dissipated heat flux

      Fid    = Fia-Fiu

      !Compute the new absorber temperature Taon

      Taon   = Tev+Fid/(Sao*Hgl_th)

      !Compute the temperature difference between the new and old values

      DFT    = dabs(Taon-Tao)

      !Check for the convergence

      if(DFT<= Tol) exit

      Tao    = Taon

      Tai    = Tao-Fiu/(Sao*Haa_cd)

      write(1,100)Real(k),Tai,Tco,DFT

10    continue
```

```fortran
      !The new temperature Tao

      Tao   = Taon

      !The new temperature Tai

      Tai   = Tao-Fiu/(Sao*Haa_cd)


      !Write(*,*)Tai,Tao,Tci,Tco

      Tfo   = Tfi+Fiu/(Mf*Cf)

      !Write(*,*)Tfo

      !Compute the conductive absorber heat flux

      Faa_cd = Haa_cd*Sao*(Tao-Tai)

      !Compute the radiative Absorber-Cover-Environment dissipated heat flux

      Fac_rd = Hac_rd*Sao*(Tao-Tci)

      !Compute the conductive absorber dissipated heat flux

      Fcc_cd = Hcc_cd*Sao*(Tci-Tco)

      !Compute the radiative Cover-Environment dissipated heat flux

      Fce_ra = Hce_ra*Sao*(Tco-Tev)

      !Compute the convective Cover-Environment dissipated heat flux

      Fce_cv = Hce_cv*Sao*(Tco-Tev)

      Write(*,*)Fiu,Faa_cd

      Write(*,*)Fid,Fac_rd,Fcc_cd,Fce_ra+Fce_cv

      Write(*,*)Tai,Tfo,Fiu/Fia

100   format(5E14.6)

      stop

      end
```
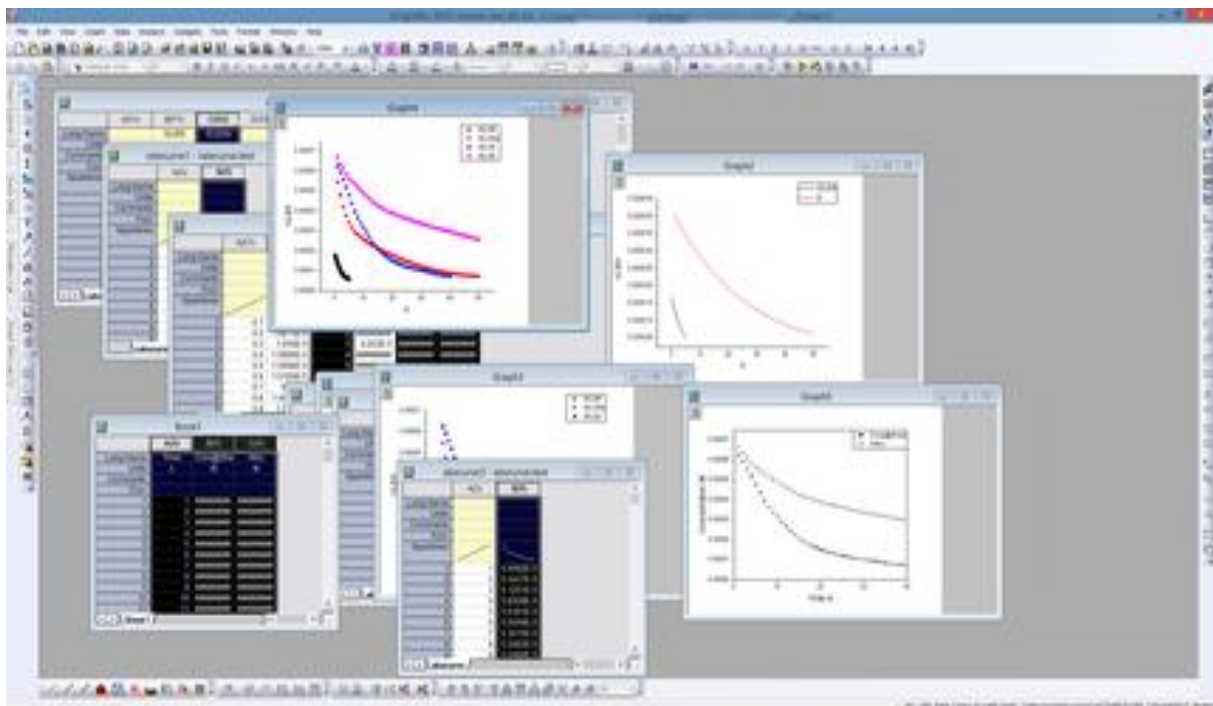
7 Presenting Origin software

Origin is a proprietary computer program well-known for its interactive capabilities in scientific graphing and data analysis. It is developed by OriginLab Corporation and is specifically designed to run on the Microsoft Windows operating system. The software has served as a source of inspiration for the creation of several open-source alternatives and clones like LabPlot and SciDAVis, which are platform-independent.

Moreover, Origin has strong graphing support with its extensive capabilities, Origin provides robust graphing support, accommodating various 2D and 3D plot types. Additionally, the software encompasses a range of data analysis capabilities, including statistical analysis, signal processing, curve fitting, and peak analysis. The curve fitting functionality within Origin utilizes a nonlinear least squares fitter, employing the well-known Levenberg-Marquardt algorithm.

Origin facilitates the import of data files in multiple formats, such as ASCII text, Excel, NI TDM, DIADem, NetCDF, SPC, and more. Furthermore, it allows users to export graphs in various image file formats, such as JPEG, GIF, EPS, TIFF, among others. For added convenience, the software incorporates a built-in query tool, enabling users to access database data efficiently.

Figure Origin interface